Applications of Spectro-Polarimetric Techniques for Imaging Plasma Flows and Current Density in Fusion Devices

Ahmed Diallo

Princeton Plasma Physics Laboratory

In Collaboration with

J. Howard[1], M. Creese[1],

S. Allen[2], R. Ellis[2], W. Meyer[2], R. Jaspers[3], J.Koning[3],

J. Chung[4], R. Boivin[5], M. Van Zeeland[5]

[1] *Plasma Research Laboratory, Australian National University*

[2] *Lawrence Livermore National Lab, CA*

[3] *FOM & TEXTOR, Germany*

[4] *KSTAR, Korea*

[5] *General Atomics DIIID, CA*

If Fusion Energy Powers the Sun,

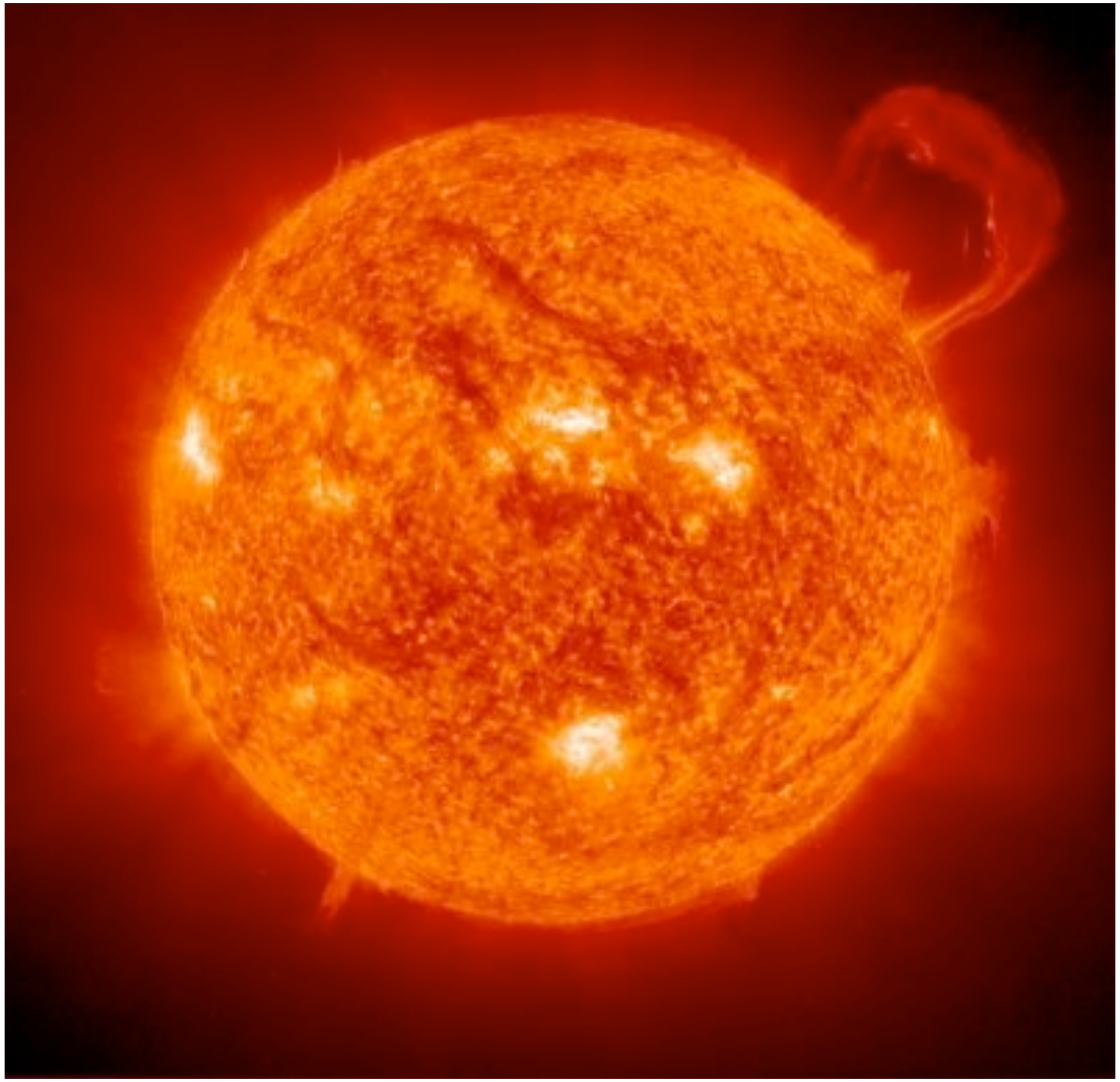

Can we make it work on Earth ?

Experiments Around the World are Investigating and Attempting to Optimize the Magnetic Configuration

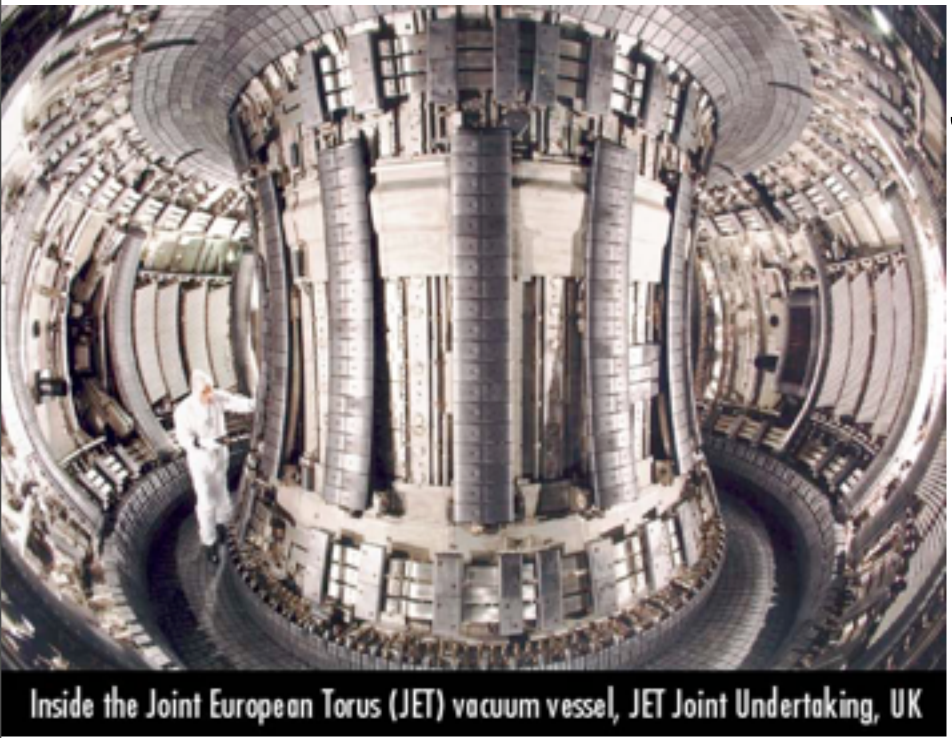

JET Tokamak

DIIID at General Atomics

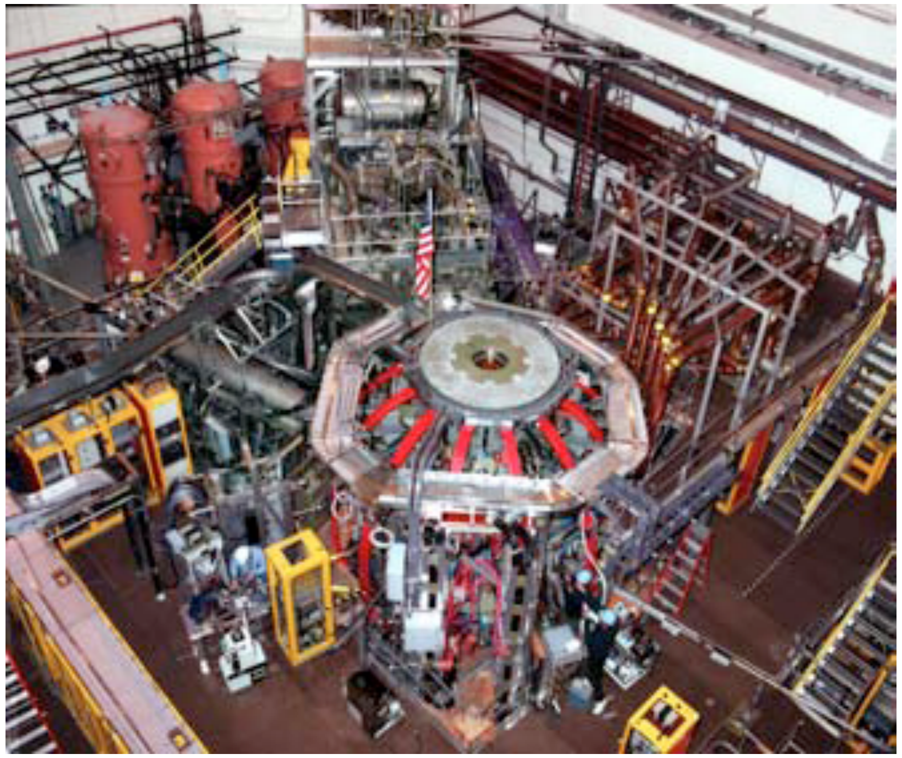

National

Spherical

Tokamak

Experiment

Textor in Germany

Experiments Around the World are Investigating and Attempting to Optimize the Magnetic Configuration

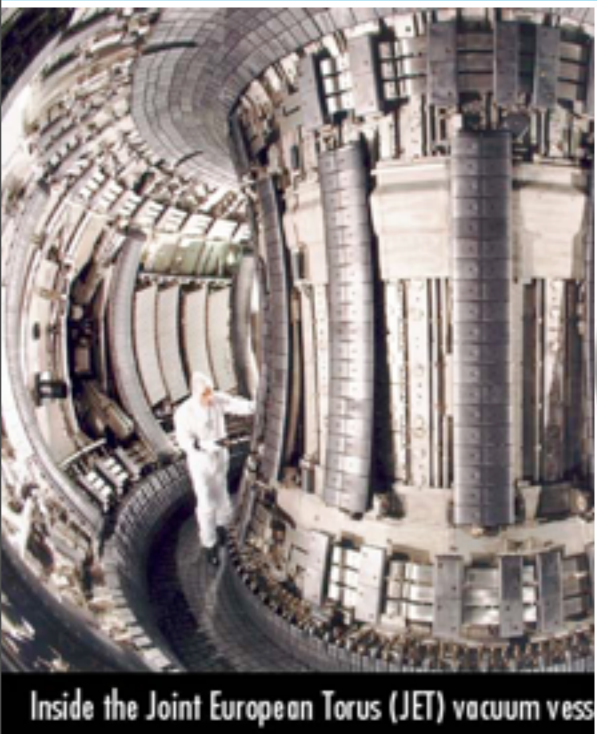

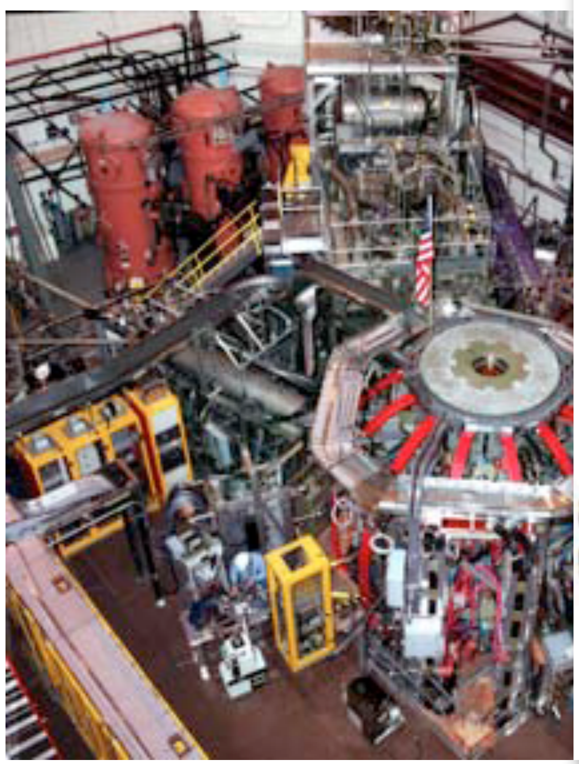

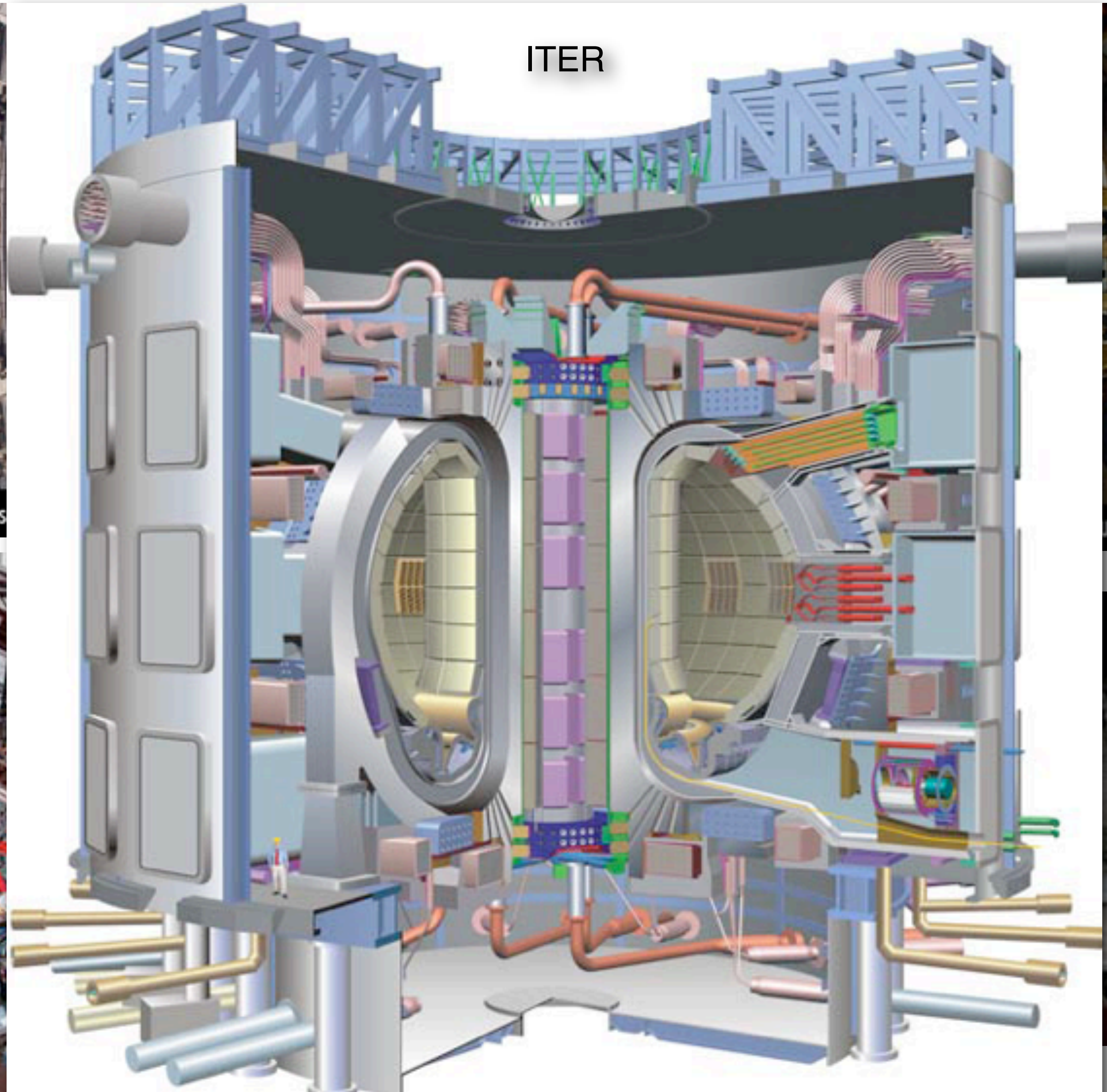

Tokamak: Helical Fields Confine Plasmas

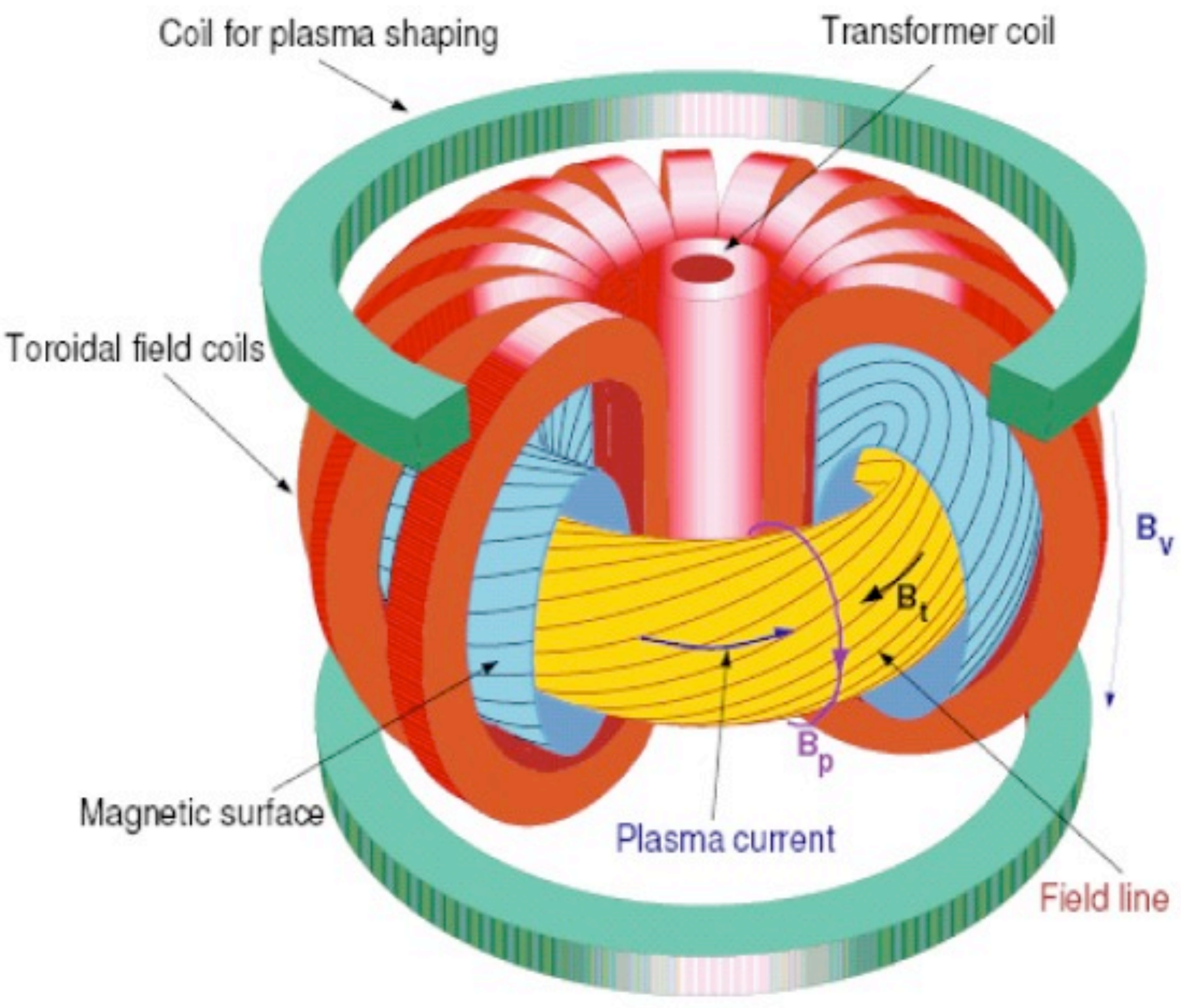

Plasma Parameters

Pulse duration up to 12 s

Plasma current 800 kA -10 MW

Magnetic field 0.5T - 3 T

Auxiliary heating 4 MW NBI, 4 MW ICRH, 500kW ECRH

Major radius 1.75 m - 2.5m

Minor radius 0.50 m - 1m

Plasma shape circular to D-shape

Density 10^{19} particles/m^3

Temperature up to 10 keV

Tokamak: Helical Fields Confine Plasmas

Plasma Parameters

Pulse duration up to 12 s

Plasma current 800 kA -10 MW

Magnetic field 0.5T - 3 T

Auxiliary heating 4 MW NBI, 4 MW ICRH, 500kW ECRH

Major radius 1.75 m - 2.5m

Minor radius 0.50 m - 1m

Plasma shape circular to D-shape

Density 10^{19} particles/m^3

Temperature up to 10 keV

Tokamak: Helical Fields Confine Plasmas

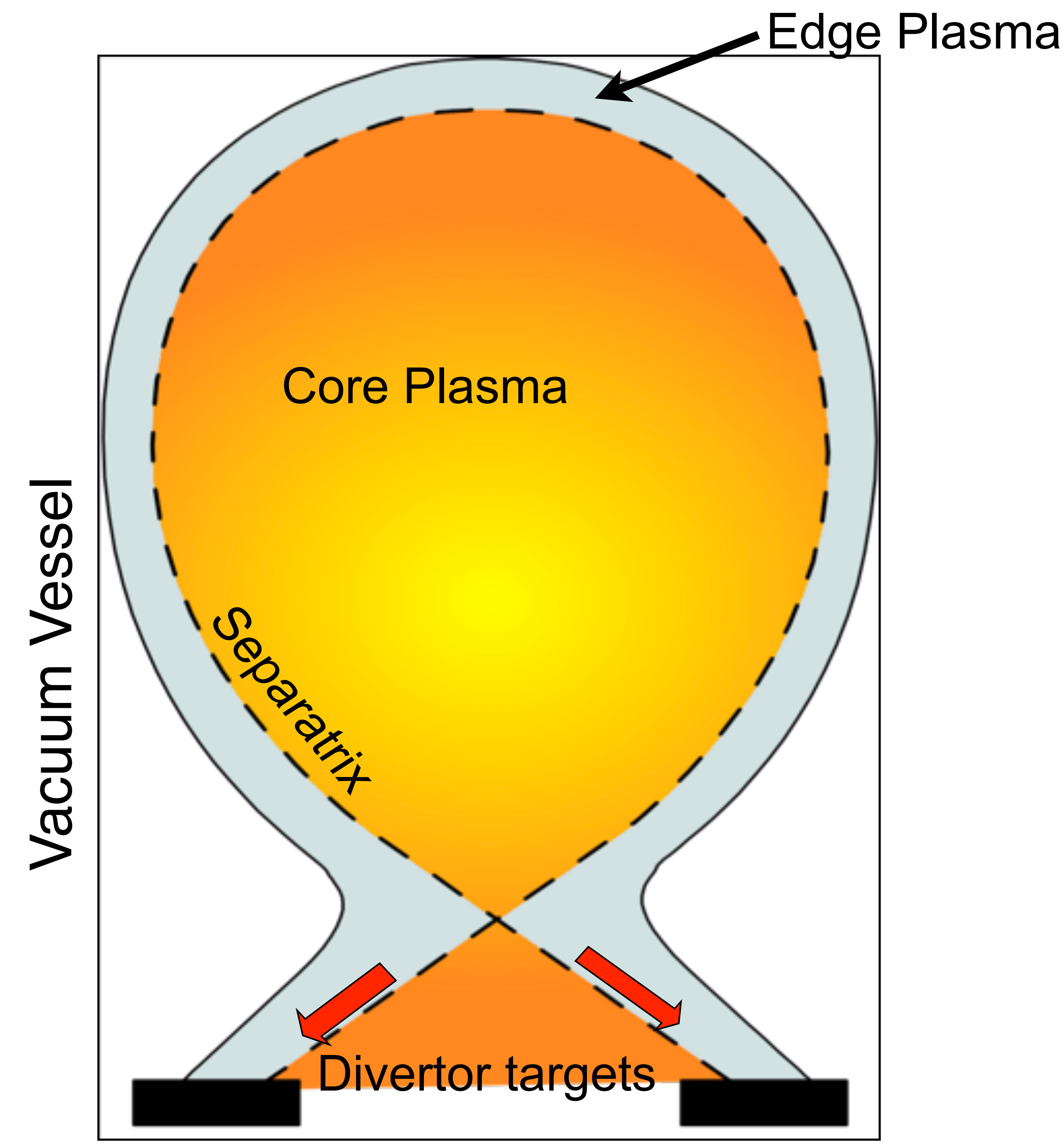

Plasma Parameters

Pulse duration up to 12 s

Plasma current 800 kA -10 MW

Magnetic field 0.5T - 3 T

Auxiliary heating 4 MW NBI, 4 MW ICRH, 500kW ECRH

Major radius 1.75 m - 2.5m

Minor radius 0.50 m - 1m

Plasma shape circular to D-shape

Density 10^{19} particles/m^3

Temperature up to 10 keV

Key Components of Plasmas Generated in a Tokamak

Fueling

Heating

Current profile

Confinement

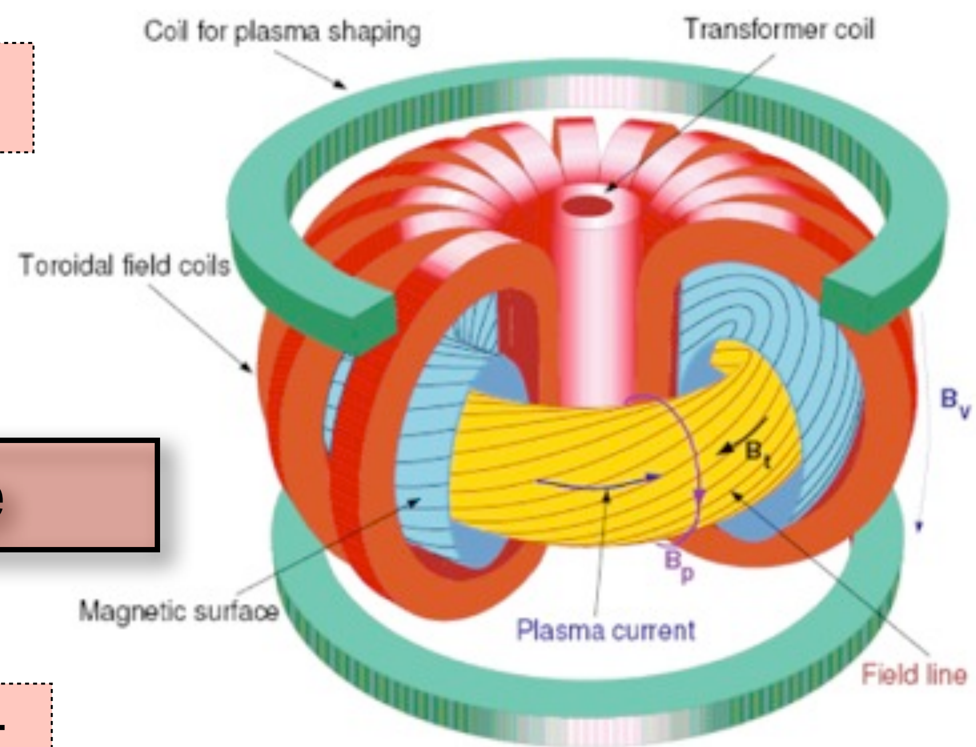

Particle exhaust

Power exhaust

Plasma Facing Component loads

Stability & transport

Impurity influx (e.g.Flows)

Core plasma

Edge plasma

Key Components of Plasmas Generated in a Tokamak

Fueling

Heating

Current profile

Confinement

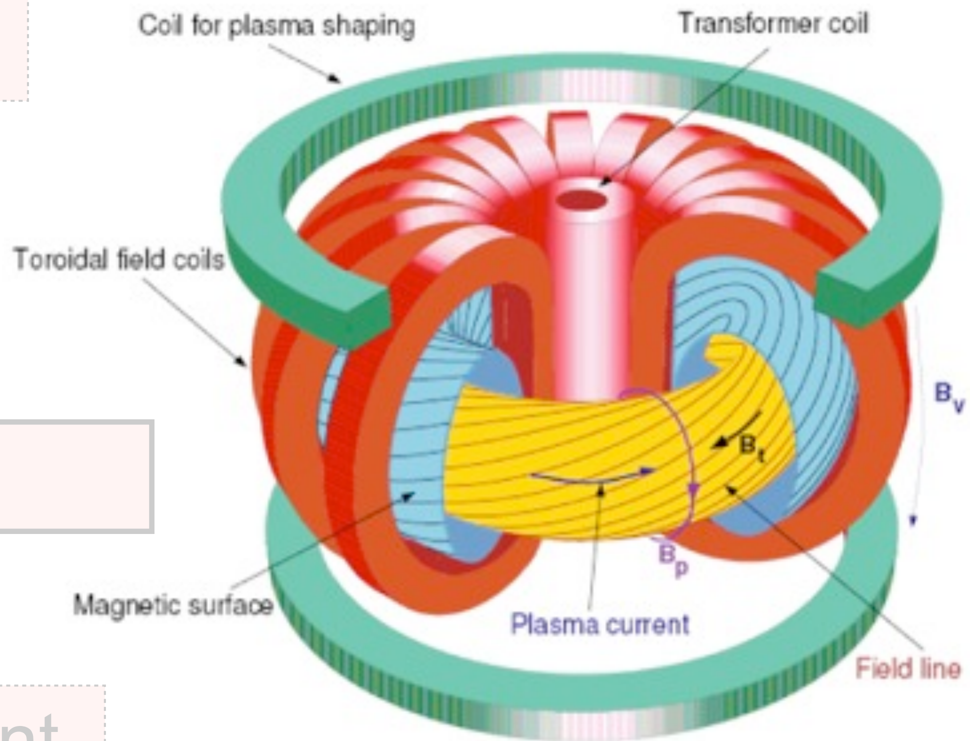

Particle exhaust

Power exhaust

Plasma Facing Component loads

Impurity influx (e.g. Flows)

Stability & transport

Core plasma

Edge plasma

Hurricane-like Flows in the Edge of Tokamaks Can Affect Plasma Performance

- Critical to measure plasma flows both in the core and the edge of confined plasmas

- Current edge flow measurement diagnostics include
    - Doppler spectroscopy - single points - poor spatial resolution
    - Mach probe - Intrusive and of limited spatial reach in plasmas

- A comprehensive picture of edge flows calls for an imaging technique
    - Larger number of lines of sight available
    - No cross calibration between detectors is required
    - Wide field of view

- Provides for detailed validations of model codes

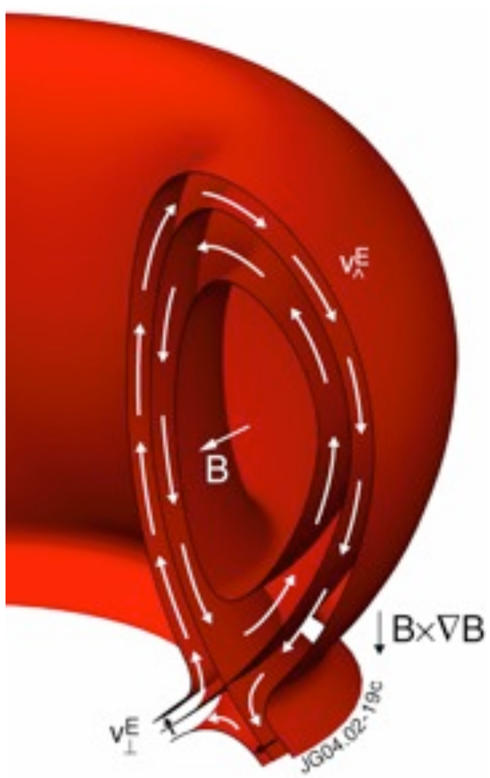

Outline

- How to image flows and the current profile?
  - Polarization interferometer
  - Spatial heterodyne system
- Applications
  - Doppler flow measurements (DIIID)
  - Magnetic field pitch angle map (TEXTOR)
- Summary and Outlook

Track Spectral Line Shift to Determine Doppler Flows

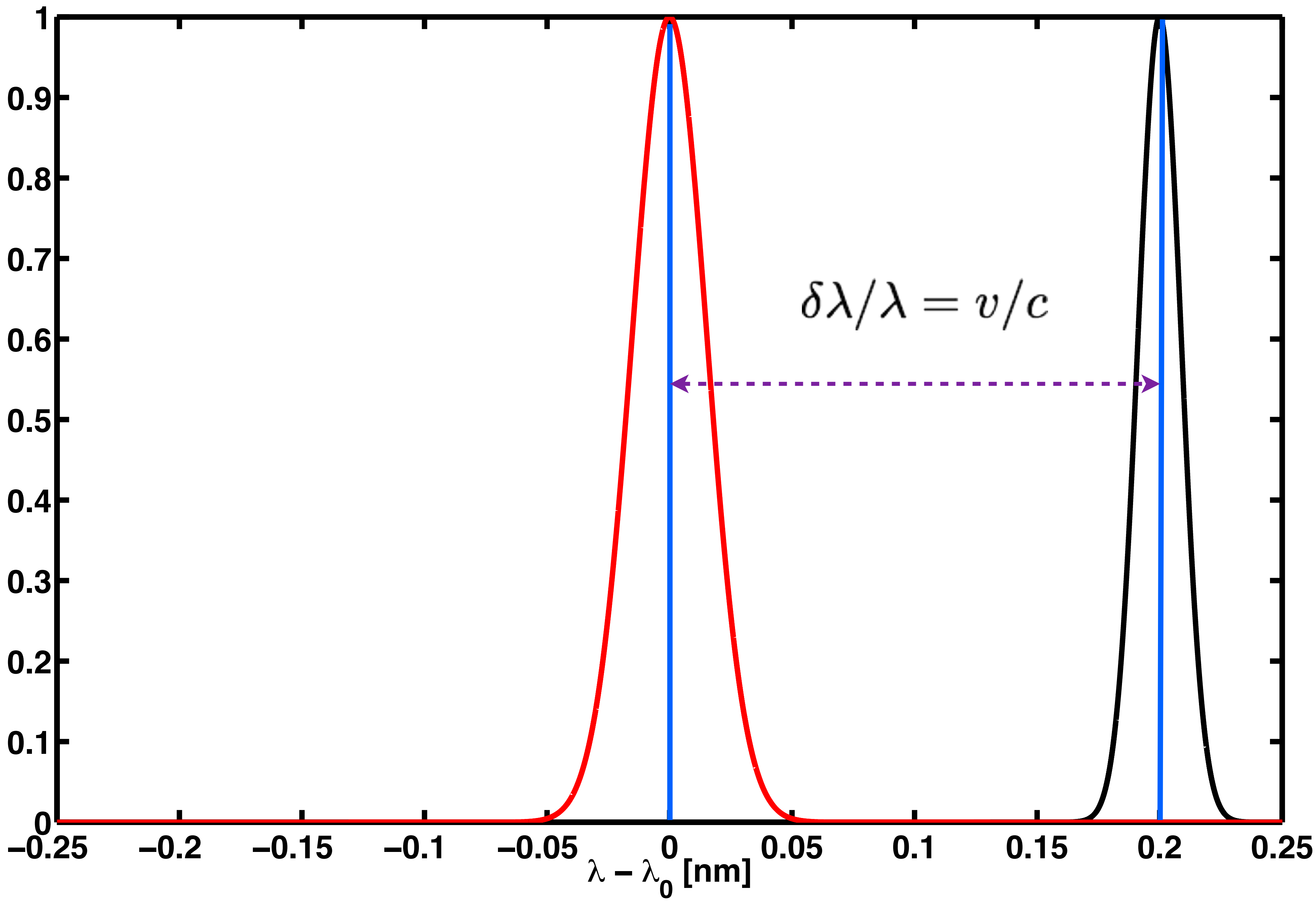

Standard Waveplate: Overview

Optical axis in the plane of incidence

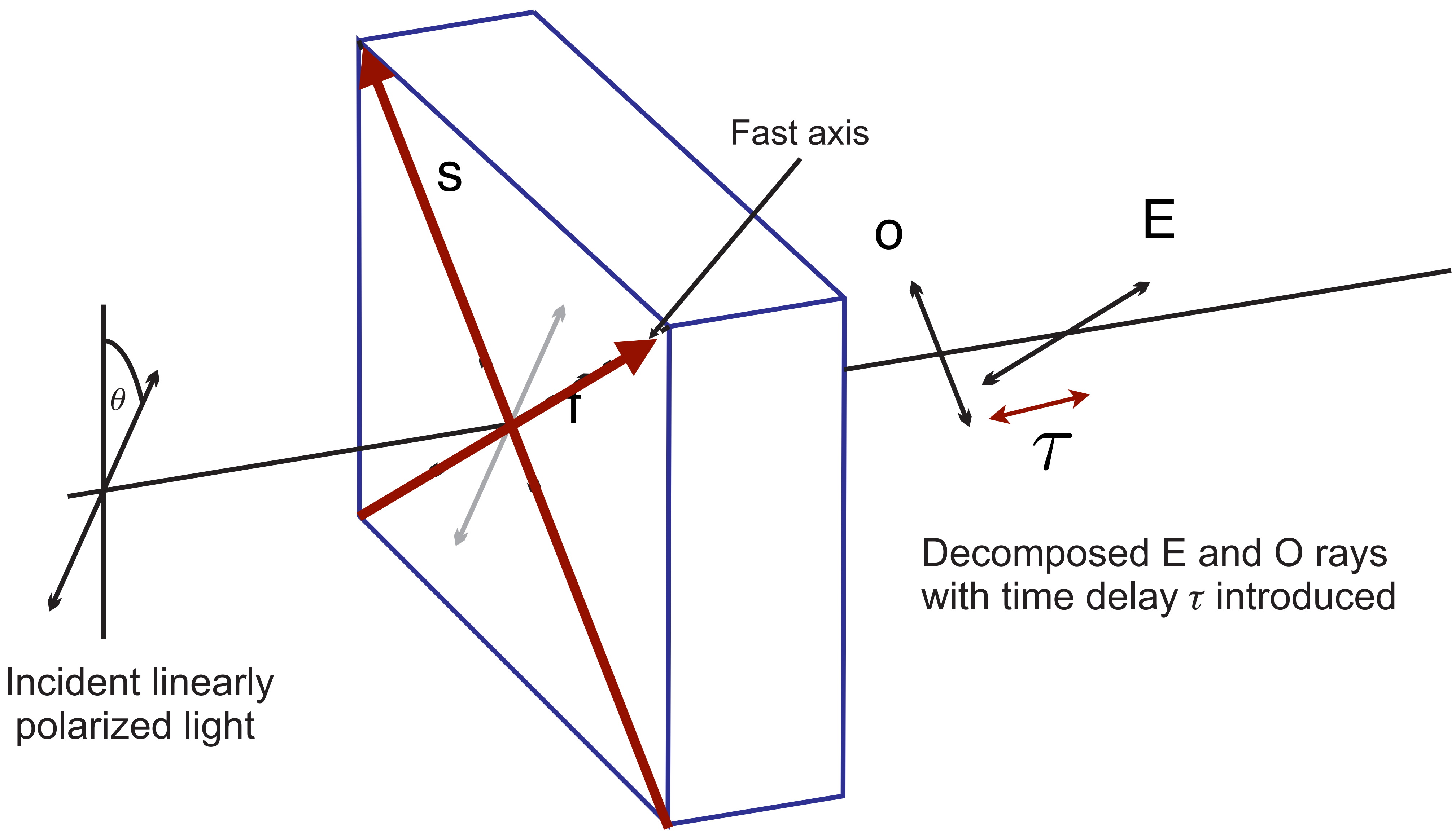

Simple Polarization Interferometer Allows for 2D Spectral Imaging

Waveplate $\varphi = \frac{2\pi|n_e(\lambda)-n_o(\lambda)|L}{\lambda}$

$$S = I(1 + \zeta cos\varphi)$$

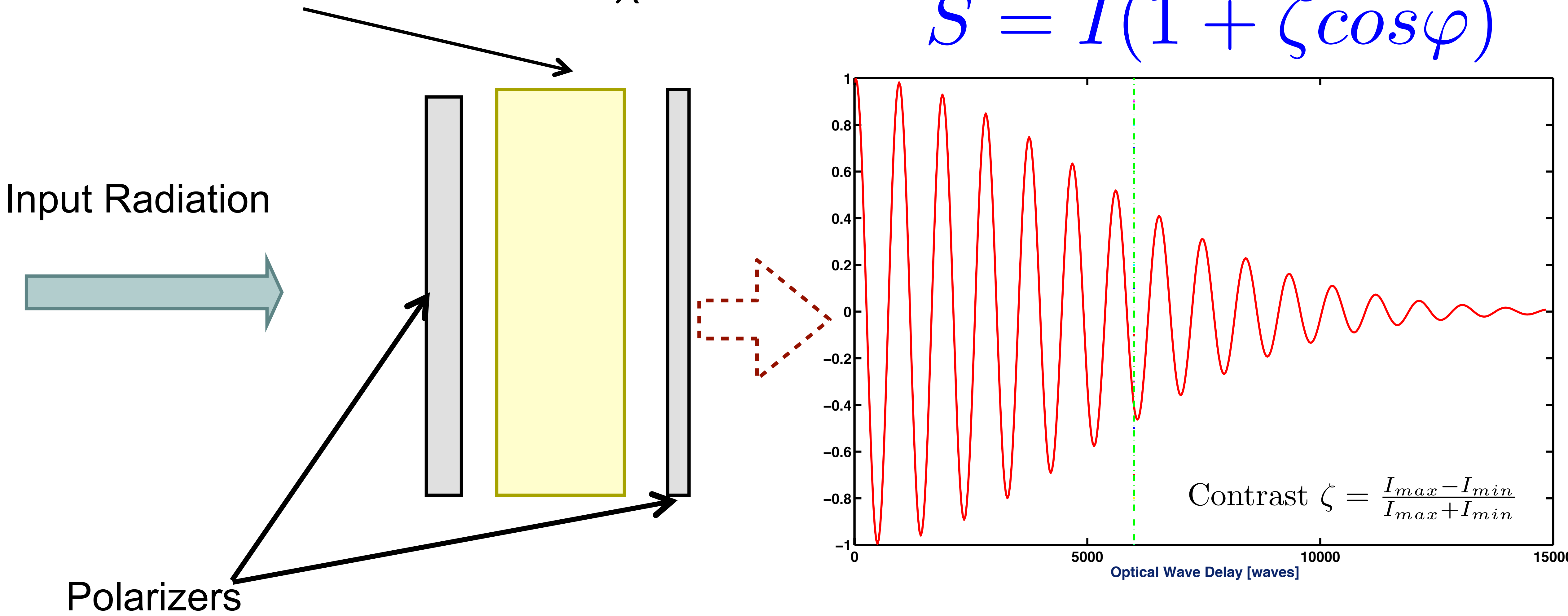

- These interferometers have higher throughput
- Requires multiplexing independent images to extract the phase shift

Generation of Spatial Fringes using a Savart Plate

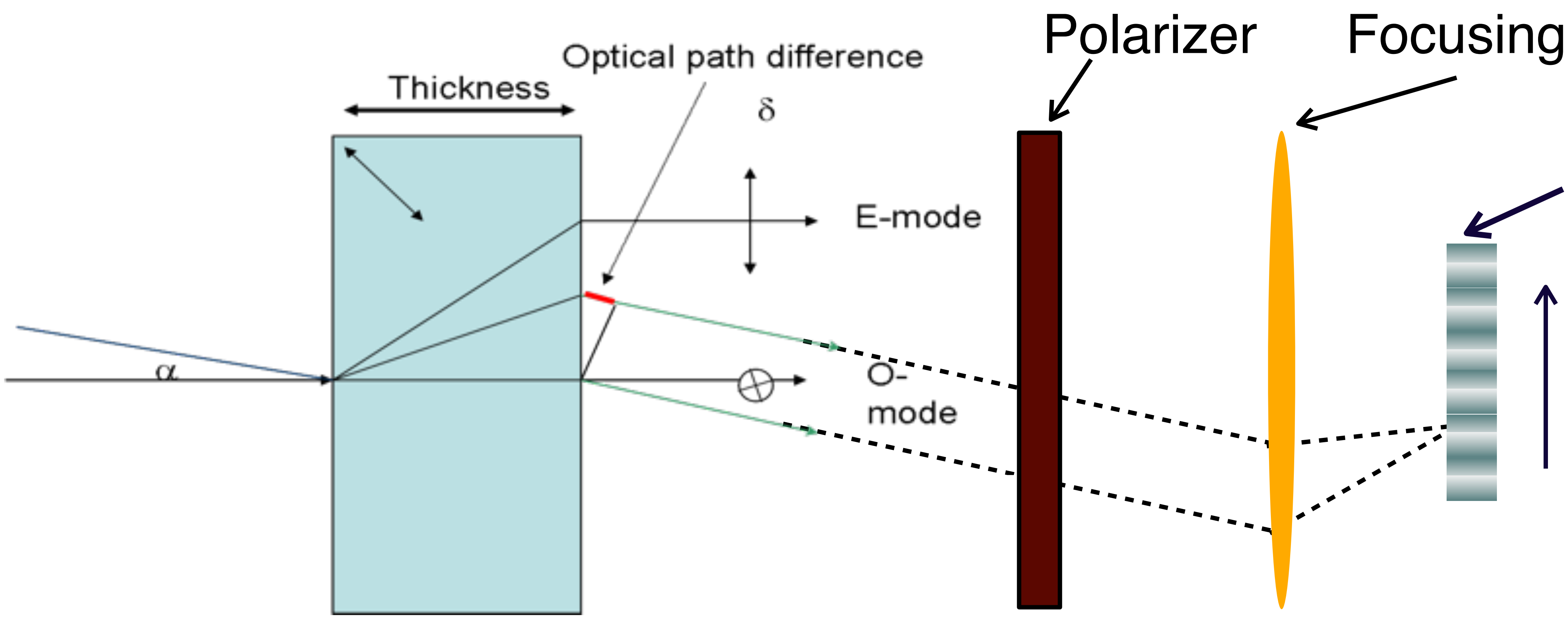

$$k = \frac{\delta}{\lambda f}$$

$$\delta = \left[A(n_e, n_o) + \frac{n_e^2 - n_o^2}{n_e^2 + n_o^2} \underbrace{\cos\eta}_{\sqrt{2}/2} \sin\alpha\right] \text{Thickness}$$

The ray separation generates an angle-dependent path difference: fringes enable spatial modulation

Shearing Polarization Interferometer: Description

Insert shearing (Savart) waveplate:

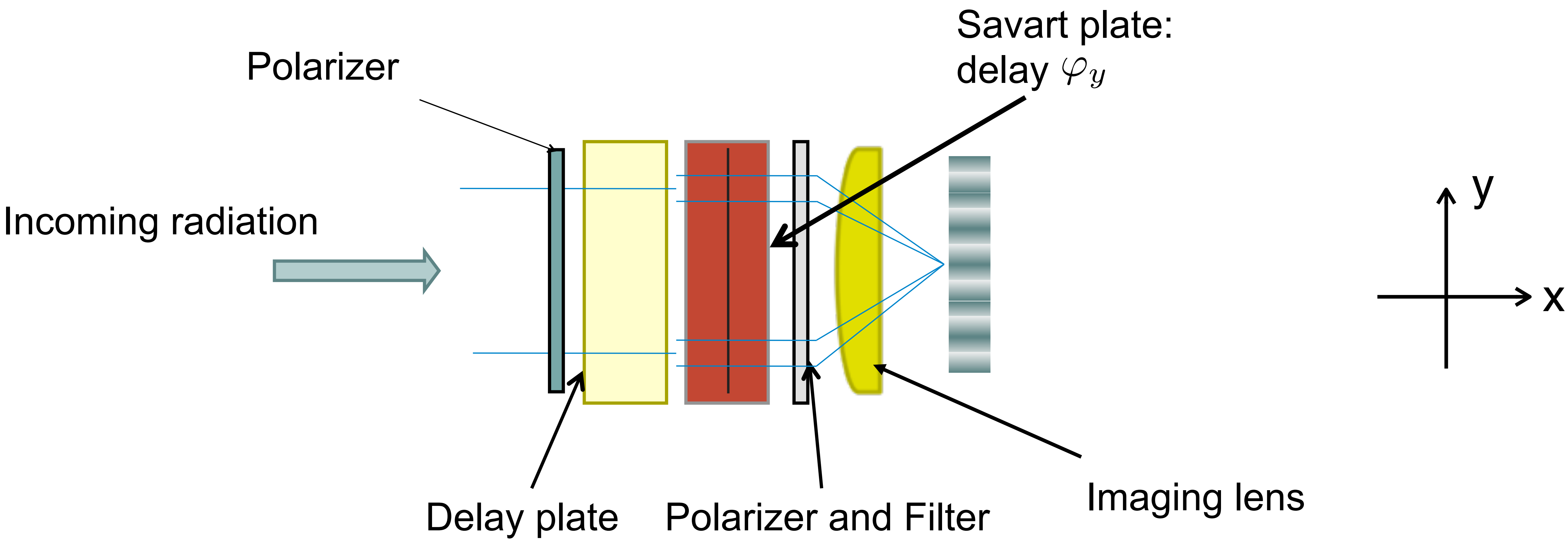

$$S = I[1 + \zeta \cos(k_y y + \varphi)]$$

Shearing Polarization Interferometer: Description

Insert shearing (Savart) waveplate:

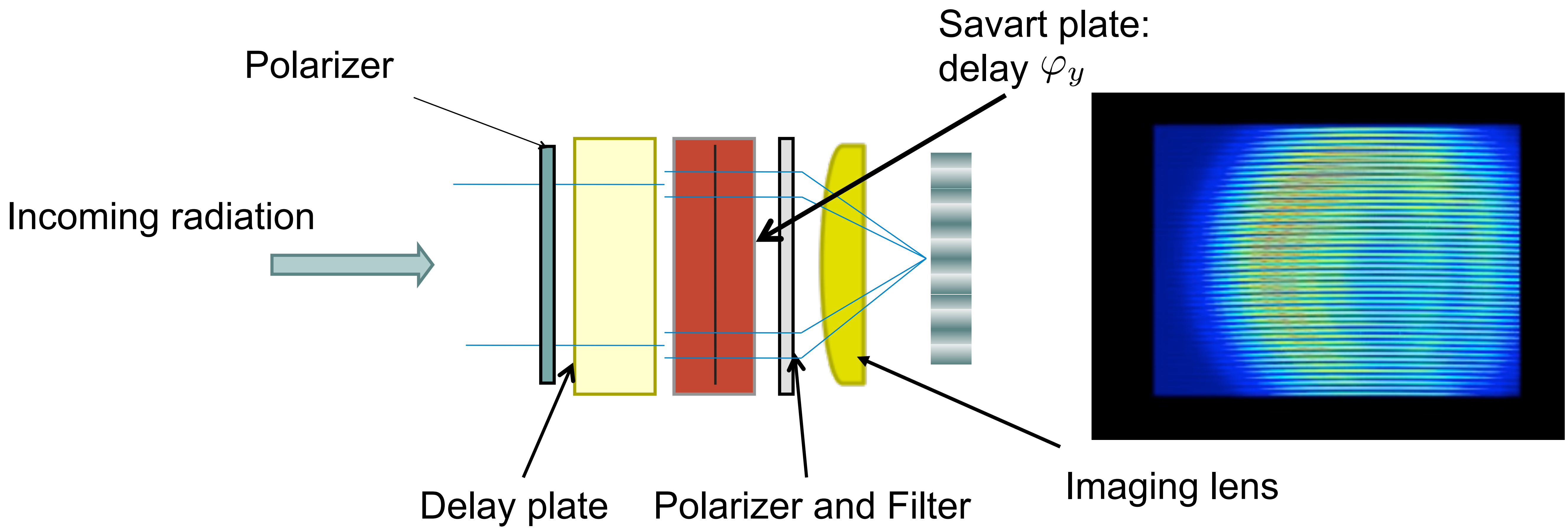

$$S = I[1 + \zeta \cos(k_y y + \varphi)]$$

Interpreting the Interferogram

- The mean interferometer signal gives the line integrated brightness:

$$S_0 = \int I_0(r) dl$$

- The fringe visibility yields the temperature:

$$< \xi >= \int I_0 \xi(r) dl \text{ where } \xi(r) = e^{-T(r)/T_{crystal}}$$

- The change in interferometer phase gives line integrated Doppler shift:

$$\frac{\delta\varphi}{\varphi} = \int I_0 \xi(r) \frac{\vec{v_0}}{c} \cdot \hat{l} dl$$

Temperature and Doppler shift of Spectral lines are Encoded on the Interferogram

Fourier Transform

Spectral Lines

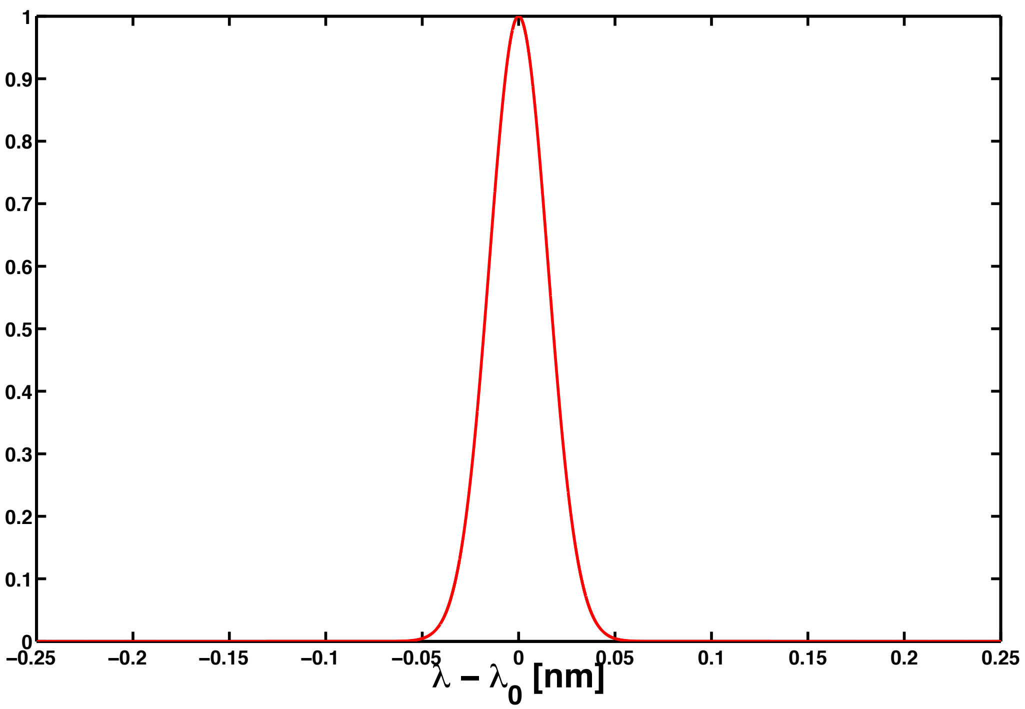

Interferogram

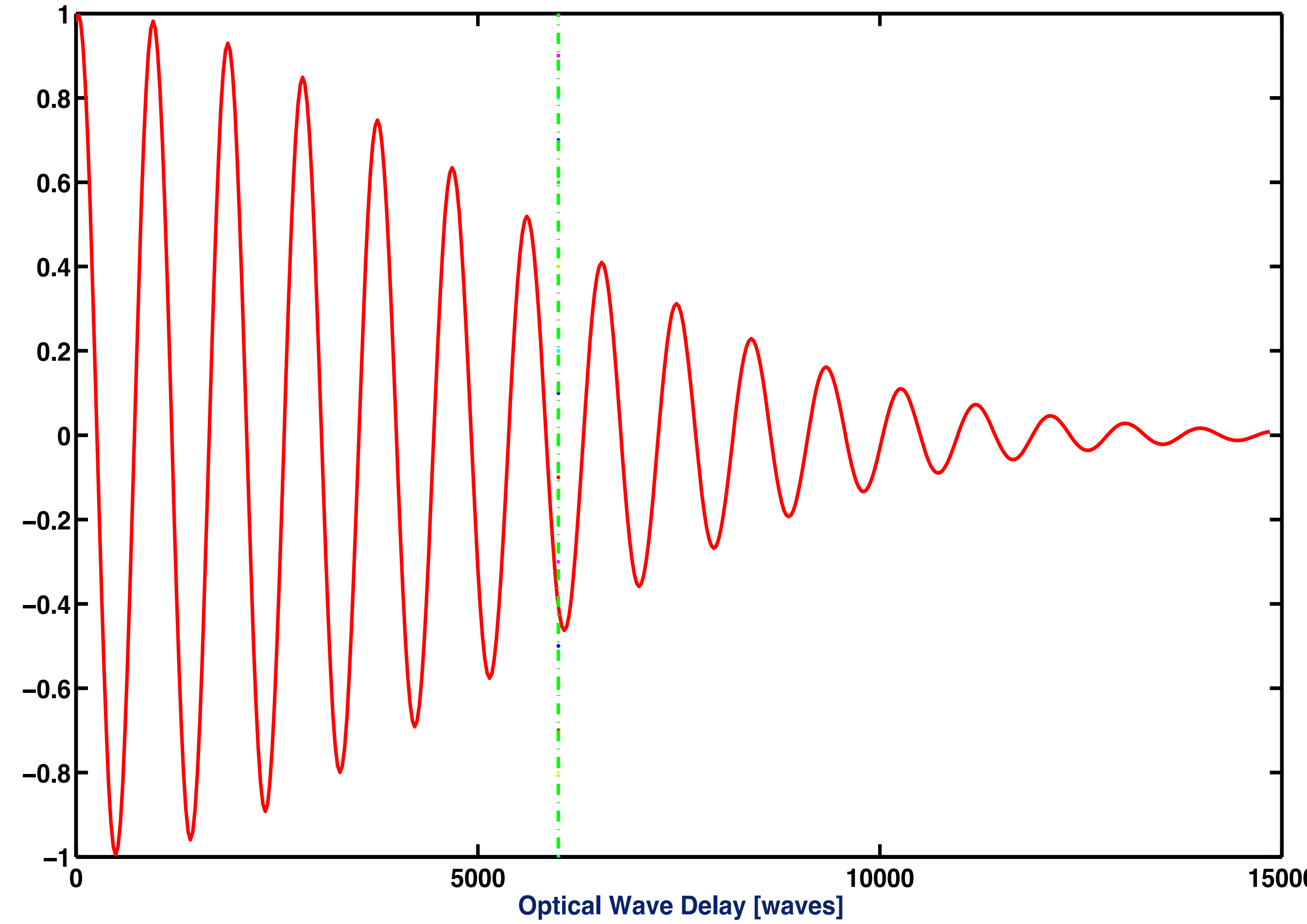

- The visibility tracks the line broadening (temperature)
- The relative phase shift is proportional to the line shift (flow)

Temperature and Doppler shift of Spectral lines are Encoded on the Interferogram

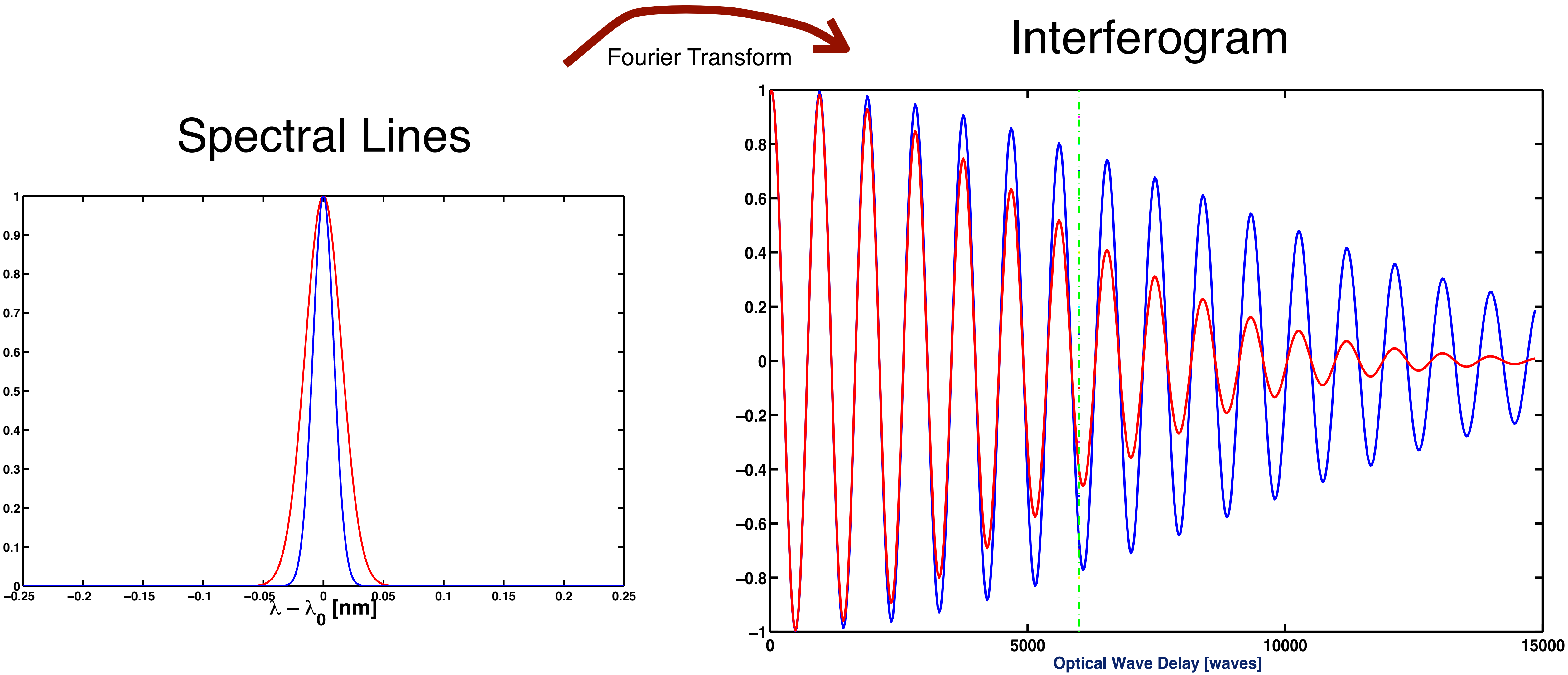

- The visibility tracks the line broadening (temperature)
- The relative phase shift is proportional to the line shift (flow)

Temperature and Doppler shift of Spectral lines are Encoded on the Interferogram

Fourier Transform

Interferogram

Spectral Lines

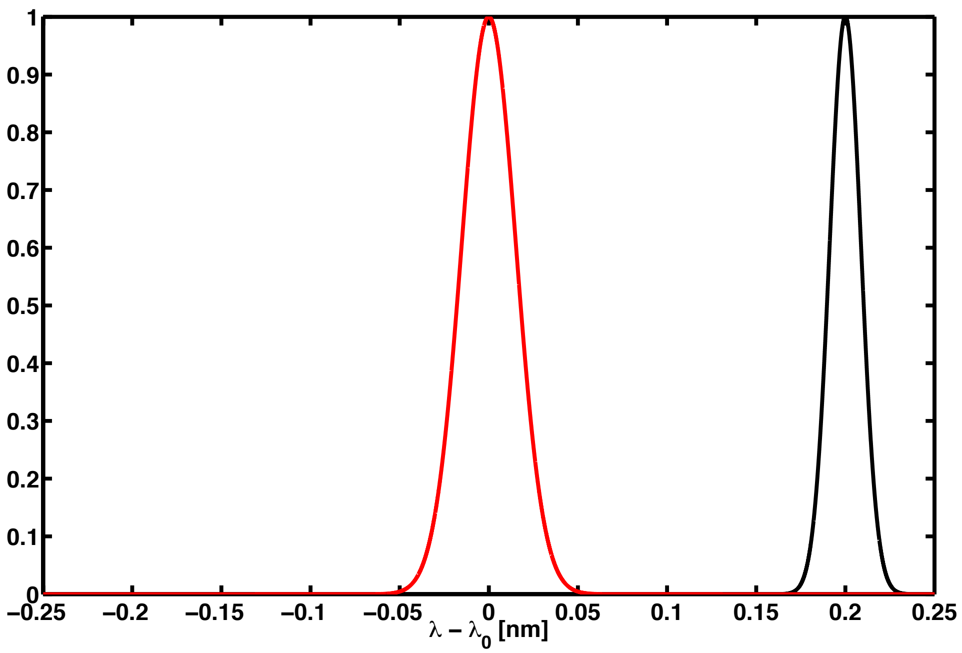

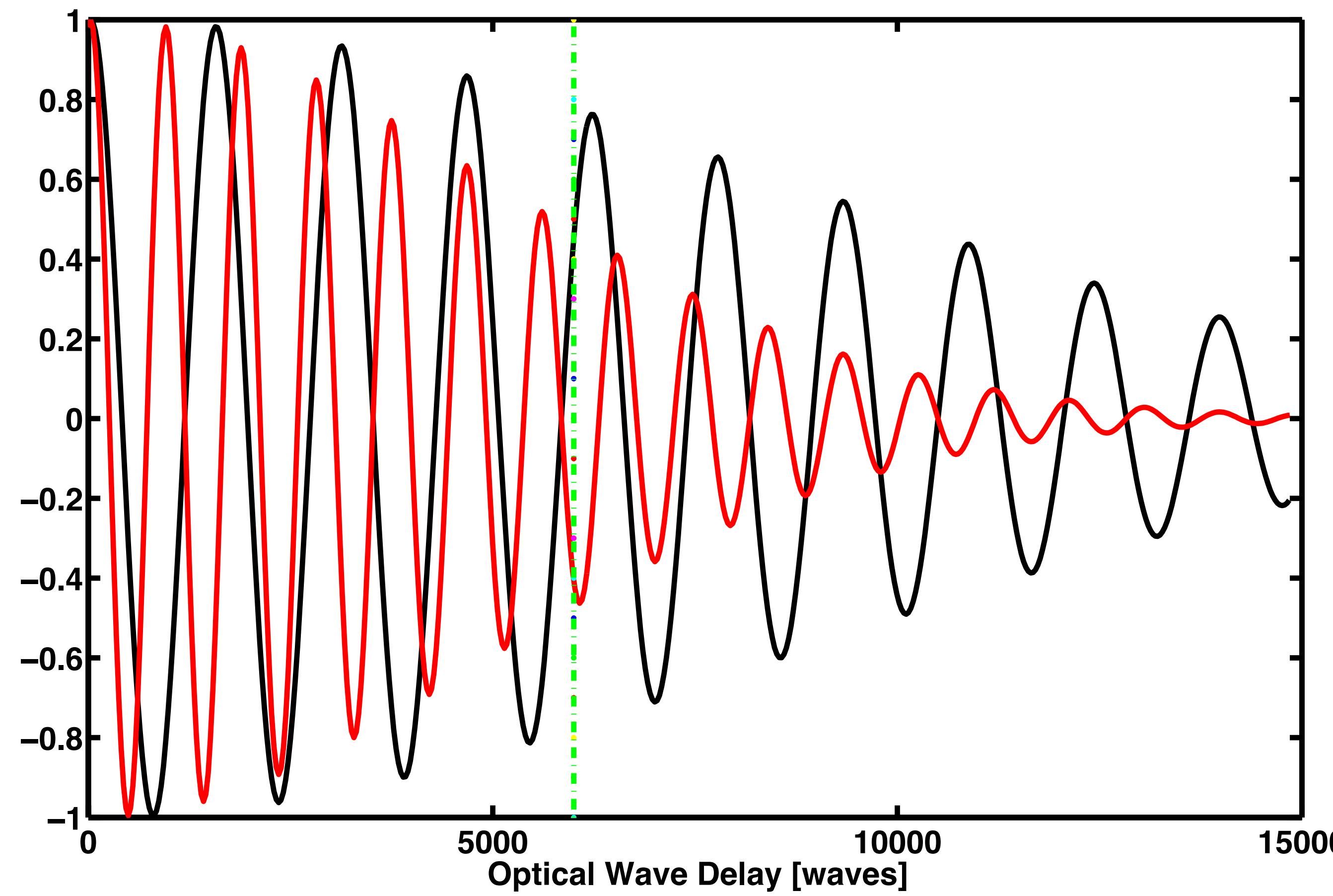

- The visibility tracks the line broadening (temperature)
- The relative phase shift is proportional to the line shift (flow)

Outline

- How to image flows and th
  - Polarization interferomet
  - Spatial heterodyne syste

Inside the DIII-D vacuum vessel, General Atomics, USA

- Applications
  - Imaging of Doppler flows (DIIID)
  - Magnetic field pitch angle map (TEXTOR)
- Summary and Outlook

Modeling CIII @ 465nm Optical Coherence: Fourier Transform of the Line Shape

Measured CIII Multiplet

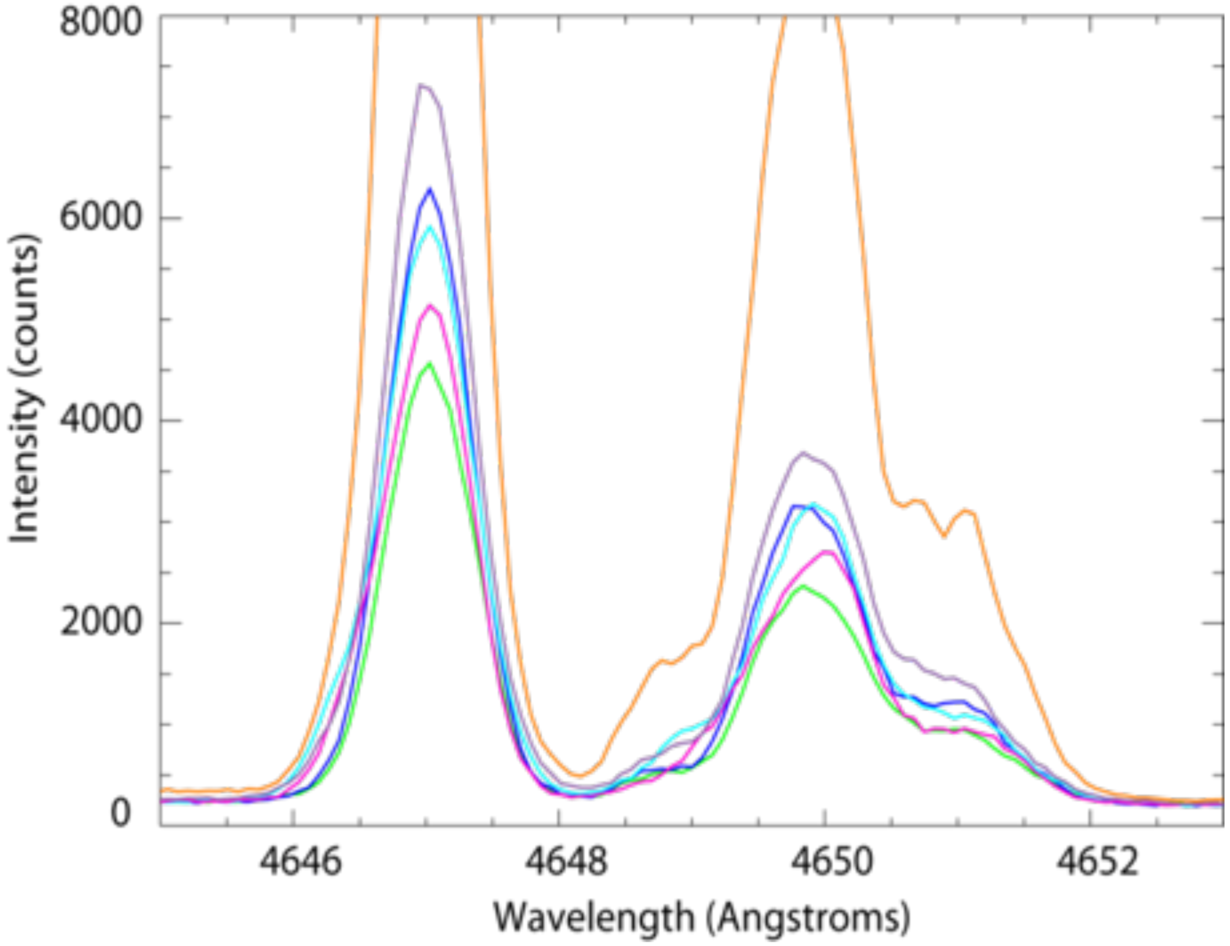

Calculated contrast

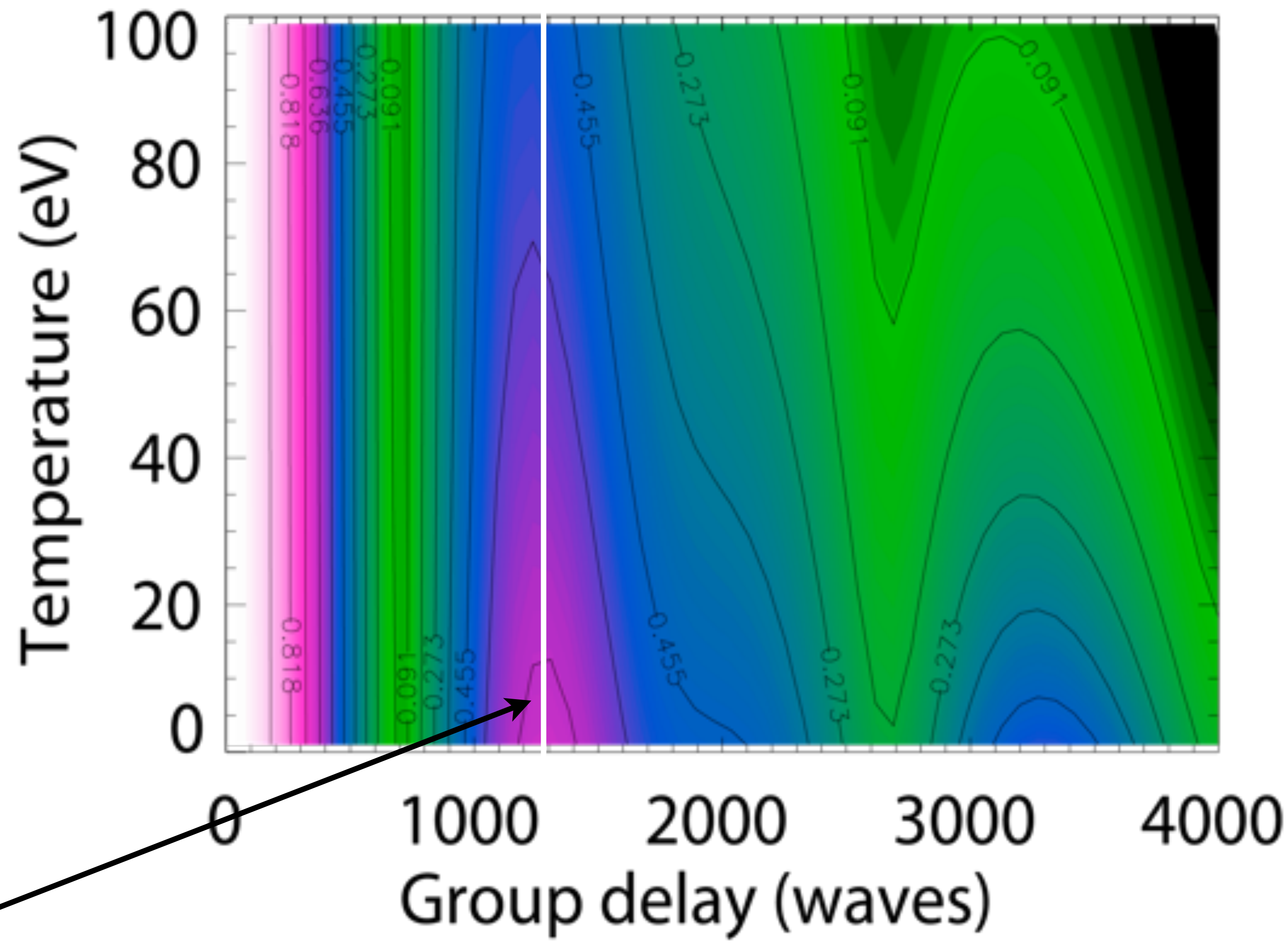

Choosing a waveplate with appropriate group delay to give sensitivity to high ion temperature

- Trade-off between group delay and contrast
- Larger wave delay improves velocity sensitivity

Measured CIII Brightness Profile is Localized at the Edge of the Plasma

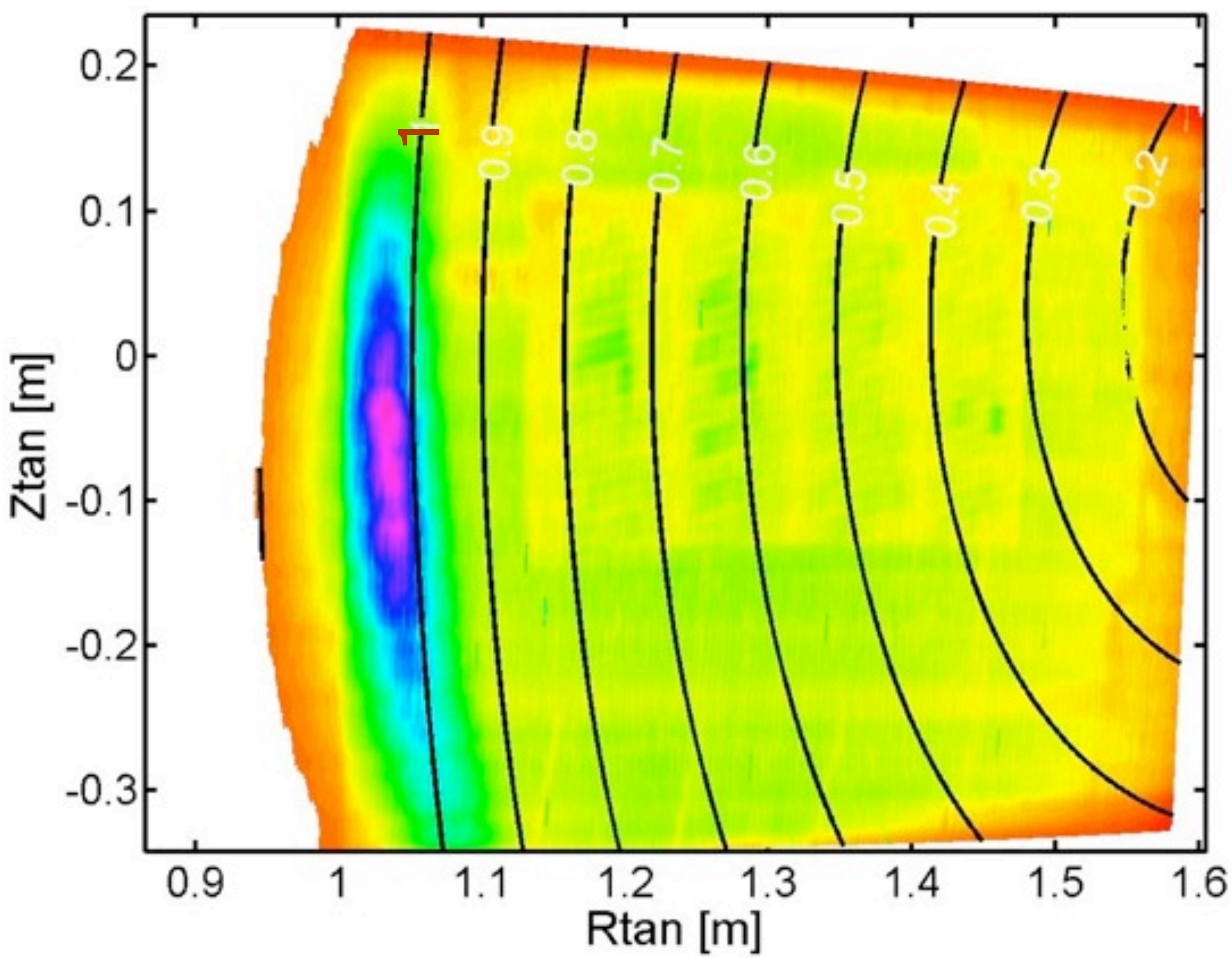

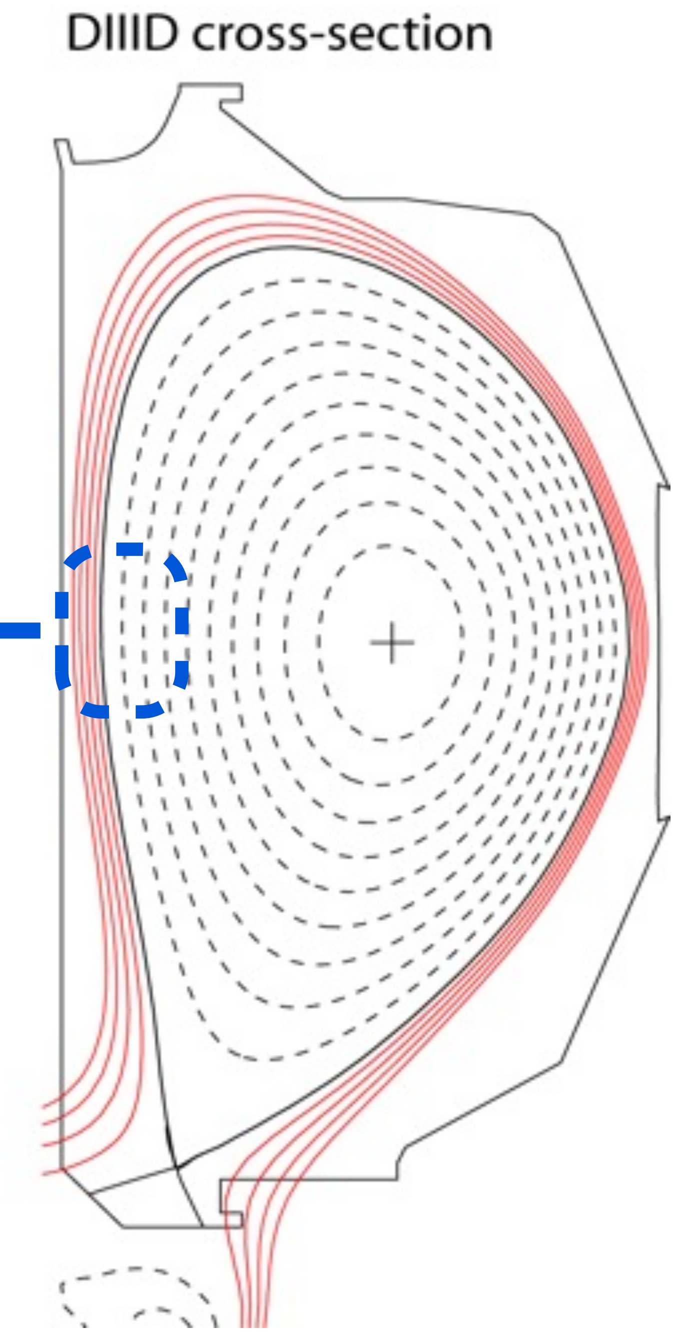

Phase Reversal Consistent with the Reversal of the Toroidal Current(Ip)

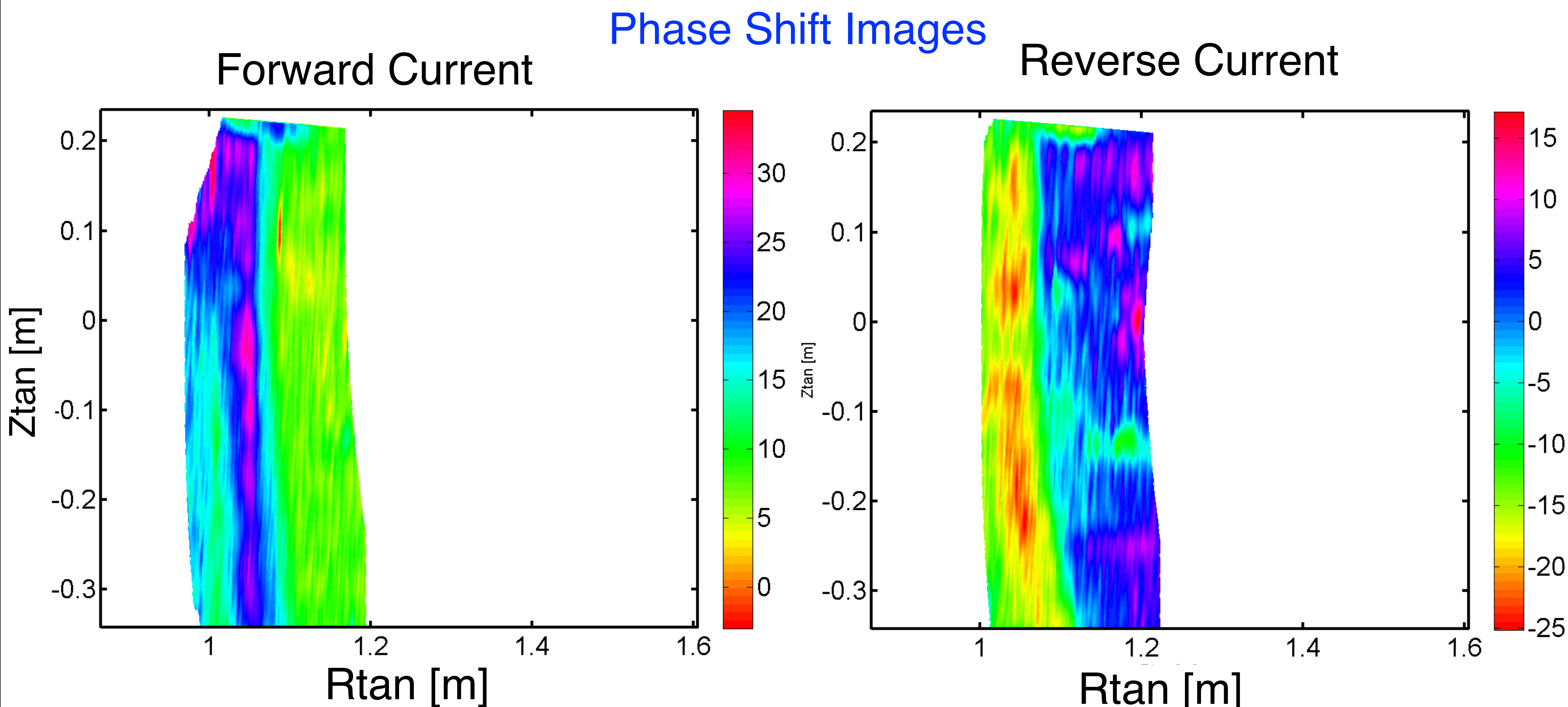

Phase Reversal Consistent with the Reversal of the Toroidal Current(Ip)

Phase Shift Images

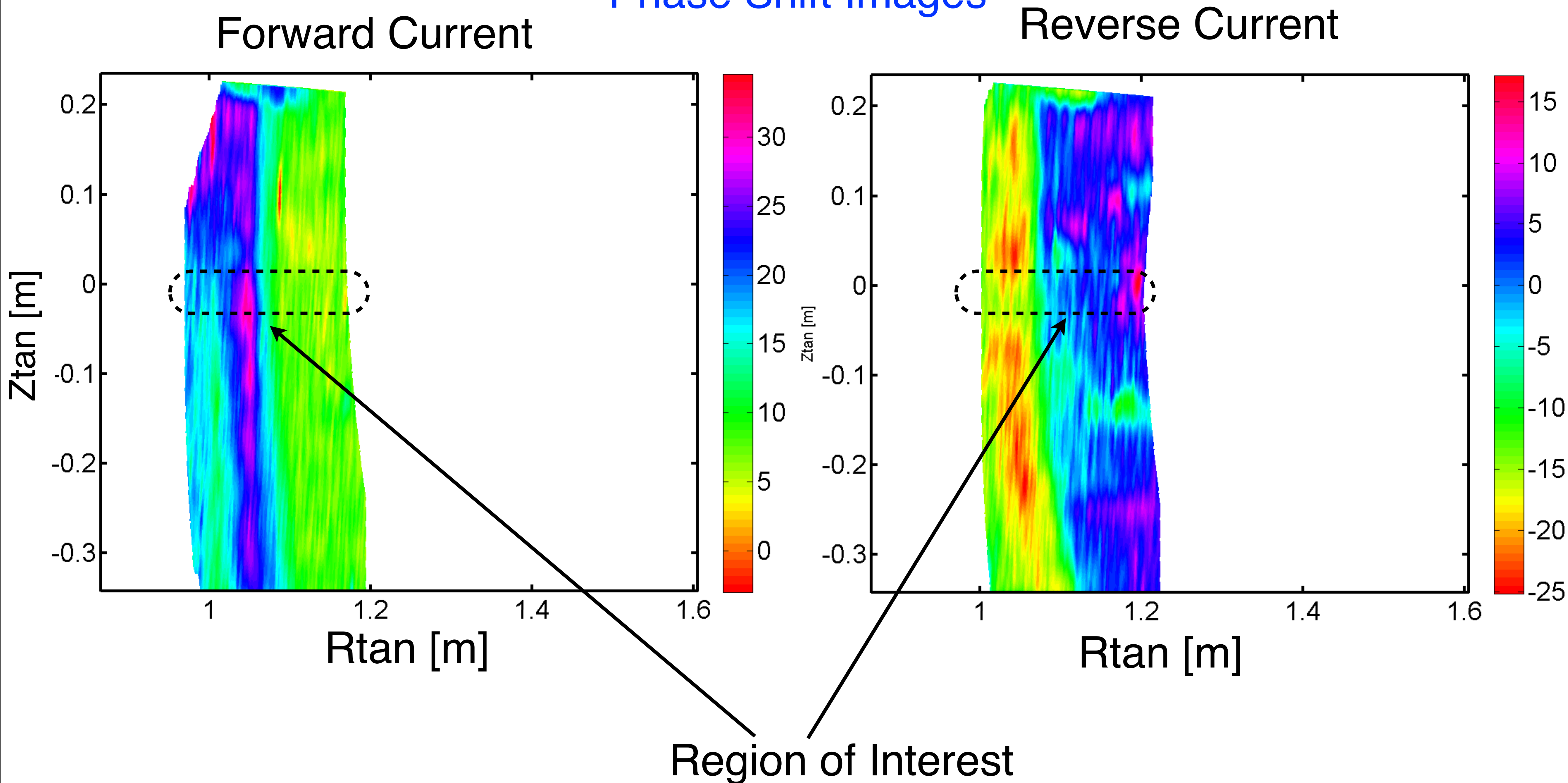

Phase Reversal Consistent with the Reversal of the Toroidal Current(Ip)

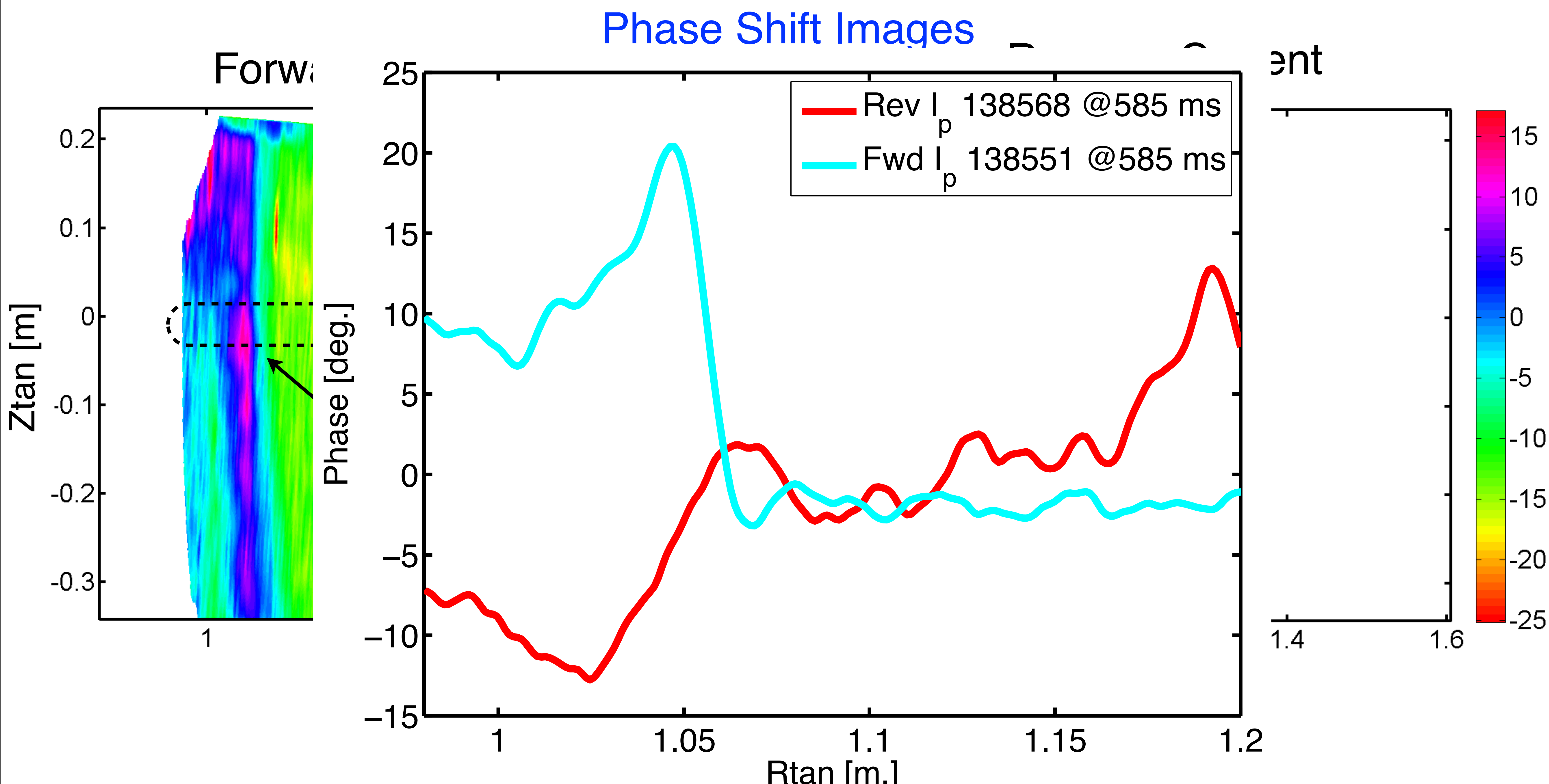

Reversal of flow agrees with other standard diagnostics

Divertor Flow Imaging Using CIII Emission

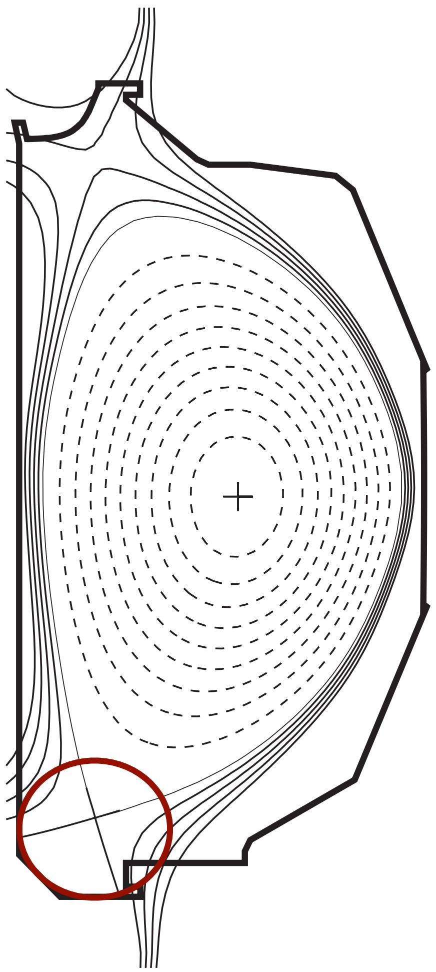

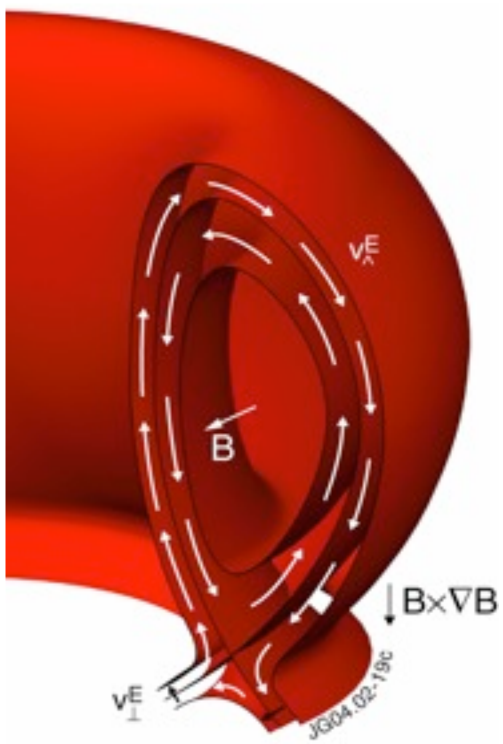

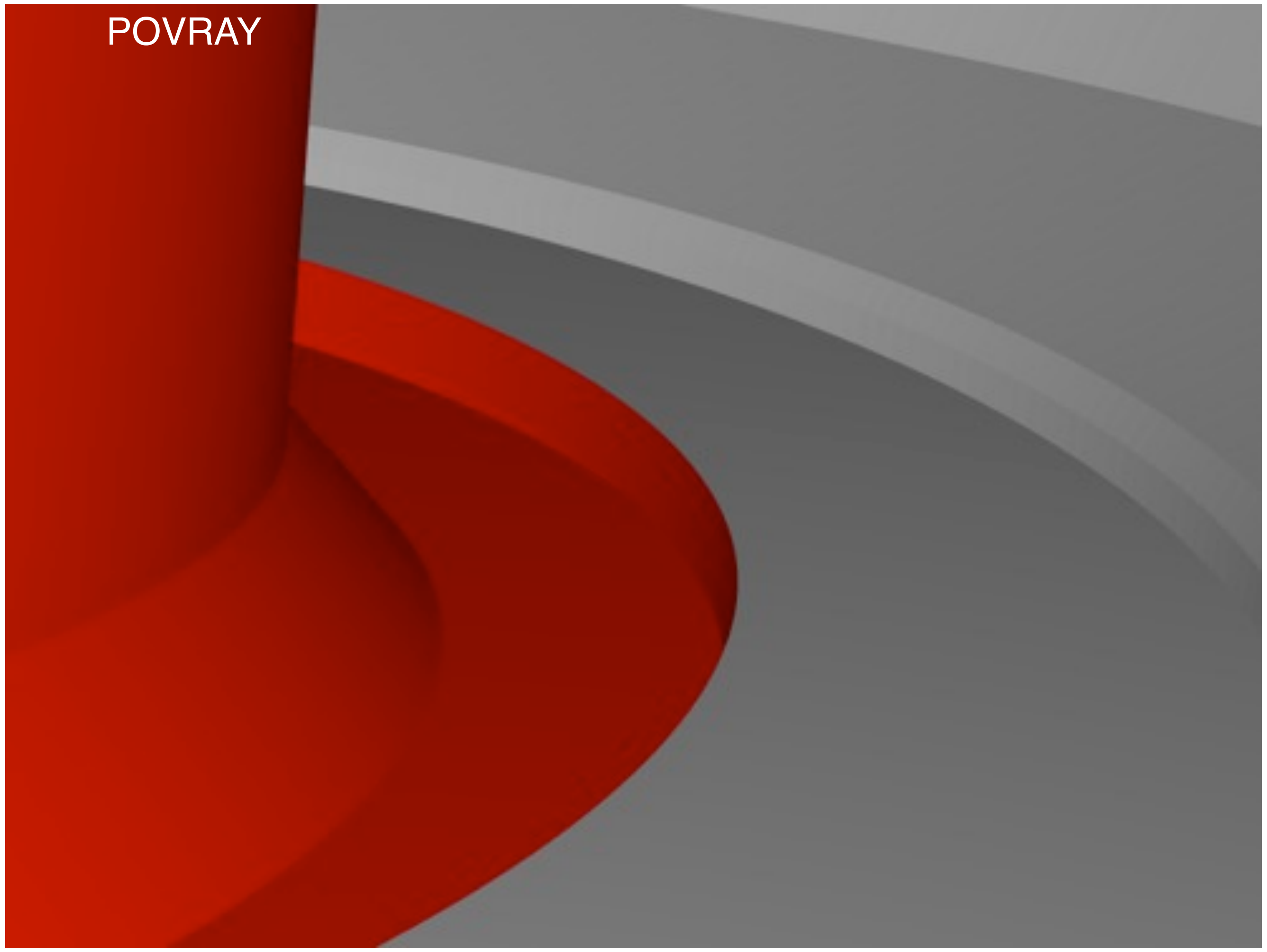

Divertor Flow Imaging Using CIII Emission

$$I = \frac{I_0}{2}[1 + \zeta cos(\varphi_y + \varphi)]$$

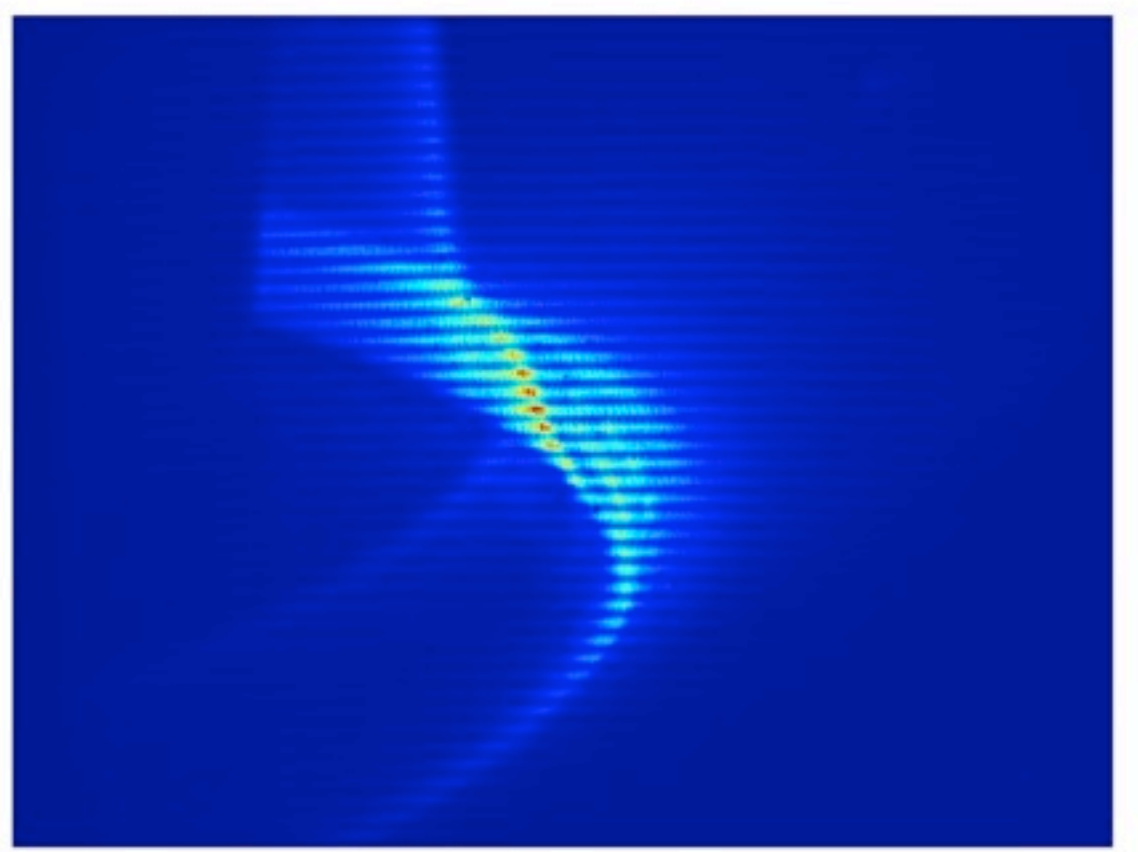

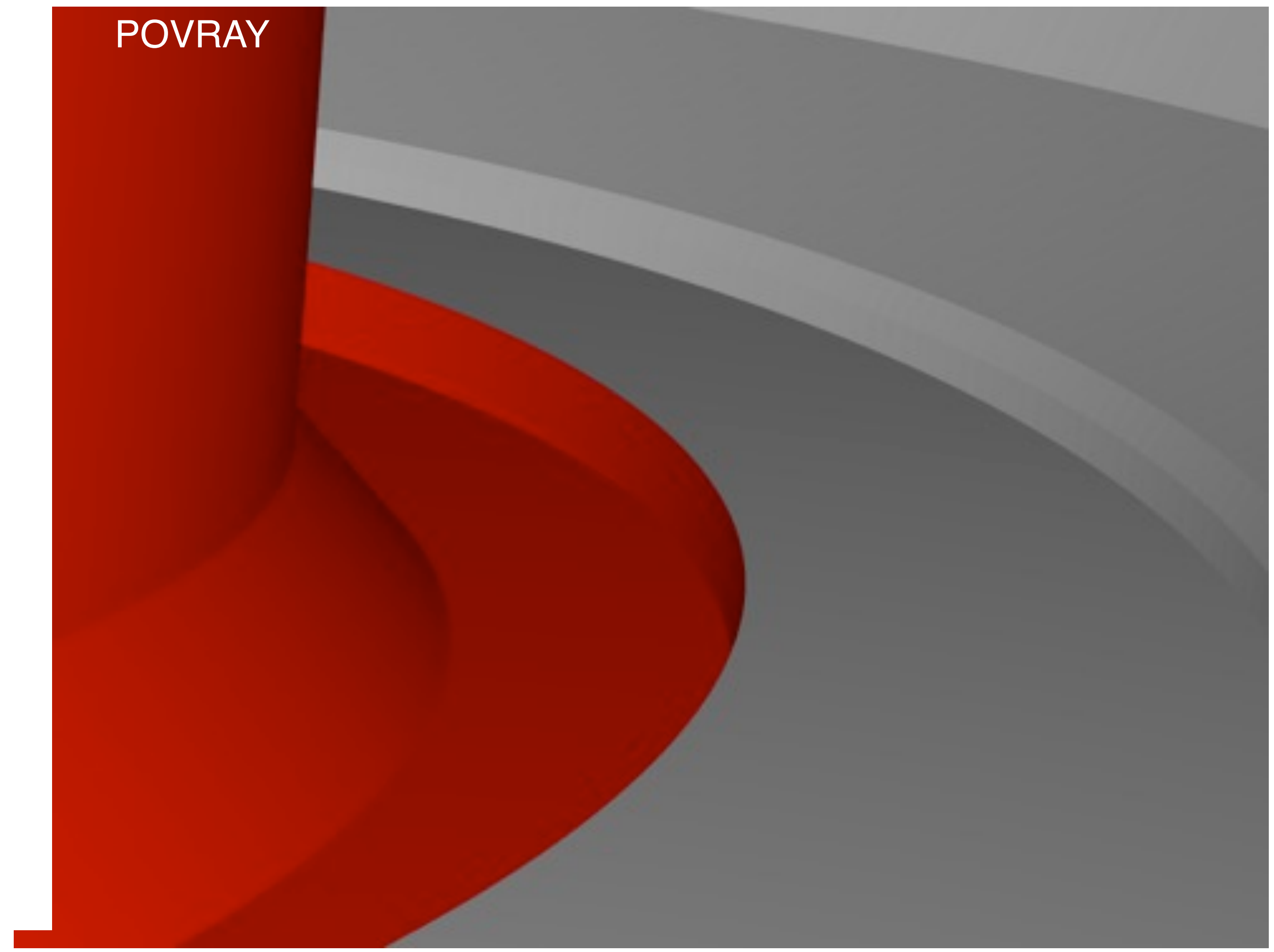

Divertor Flow Imaging Using CIII Emission

$$I = \frac{I_0}{2}[1 + \zeta cos(\varphi_y + \varphi)]$$

$$\vec{v} \cdot \hat{l} = \frac{\delta\varphi_{max}}{\kappa\varphi_0} c \sim 27\ km.s^{-1}$$

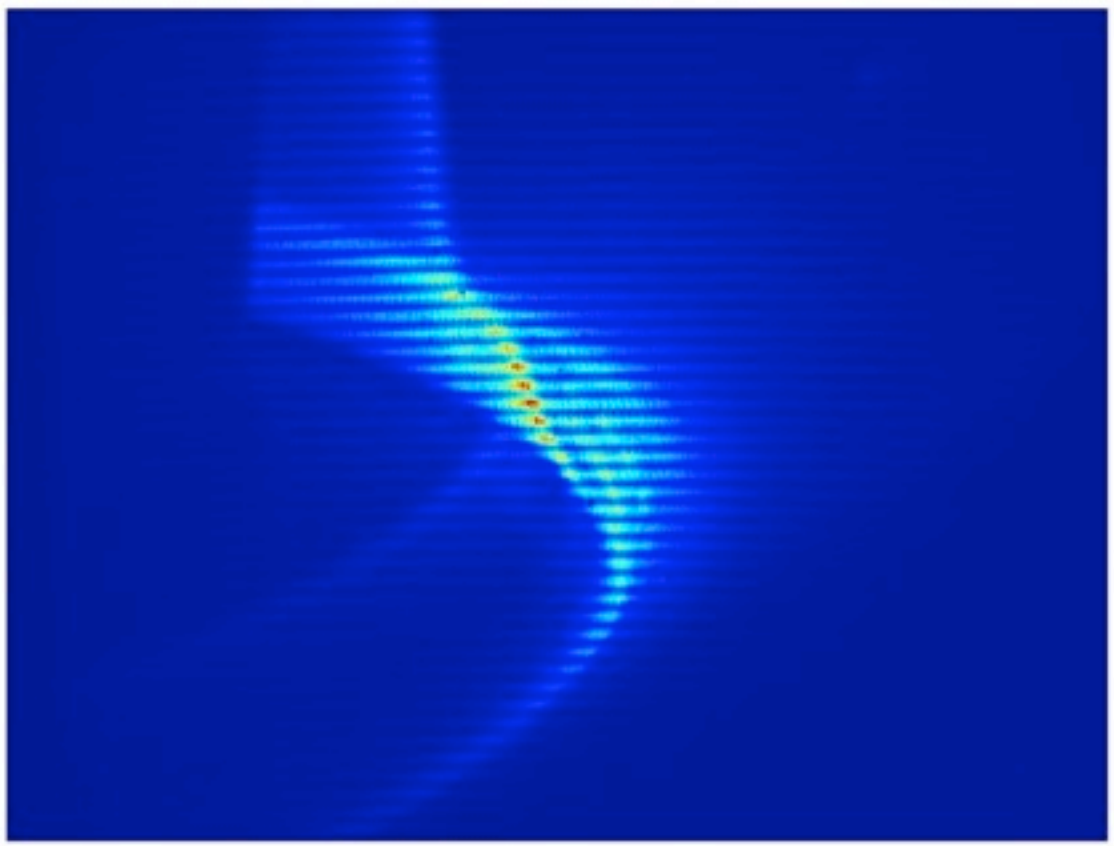

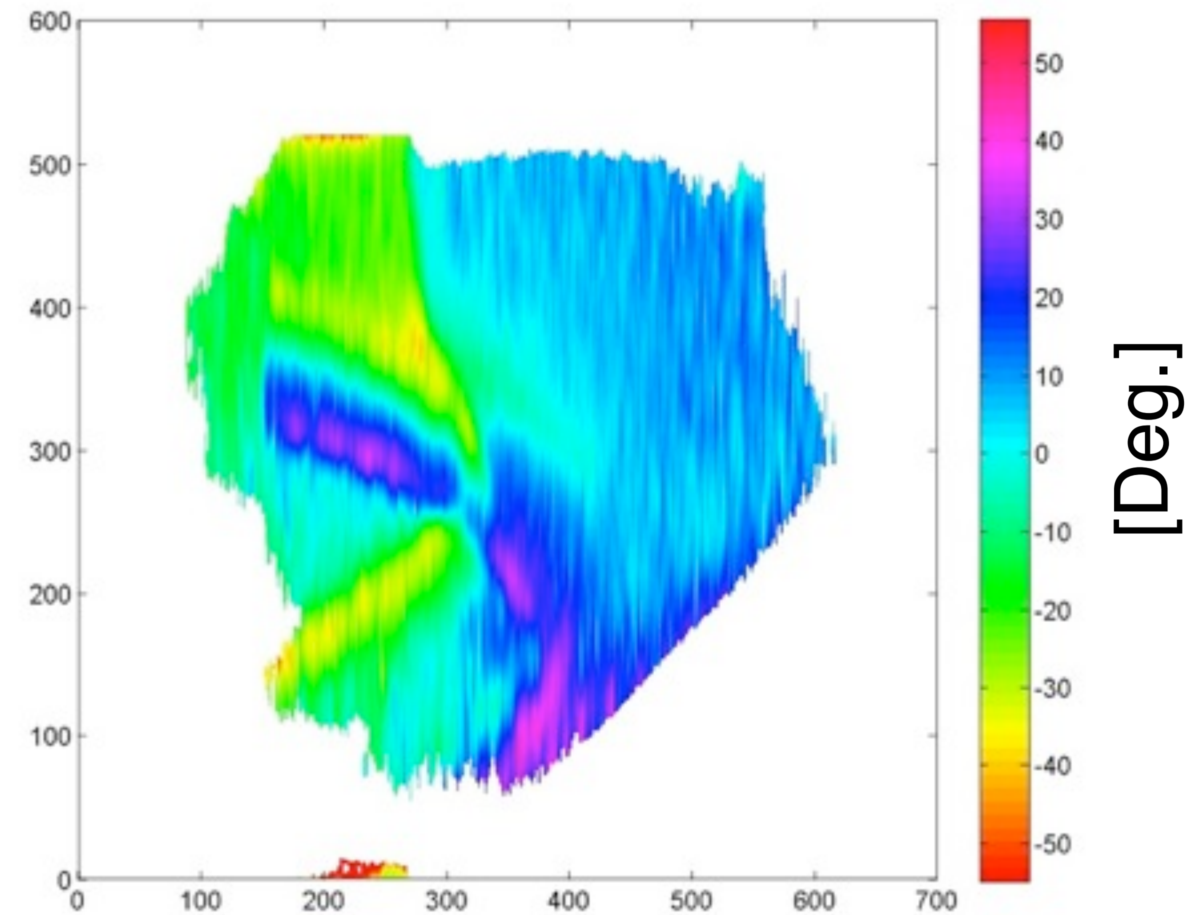

Complex flow pattern structure requires a 3D unfolding!

Movie Showing the Time Evolution of Divertor Flow Pattern

Raw Image

Demodulated Image: Phase shift

#140570 Exposure 50 ms

Movie Showing the Time Evolution of Divertor Flow Pattern

Raw Image

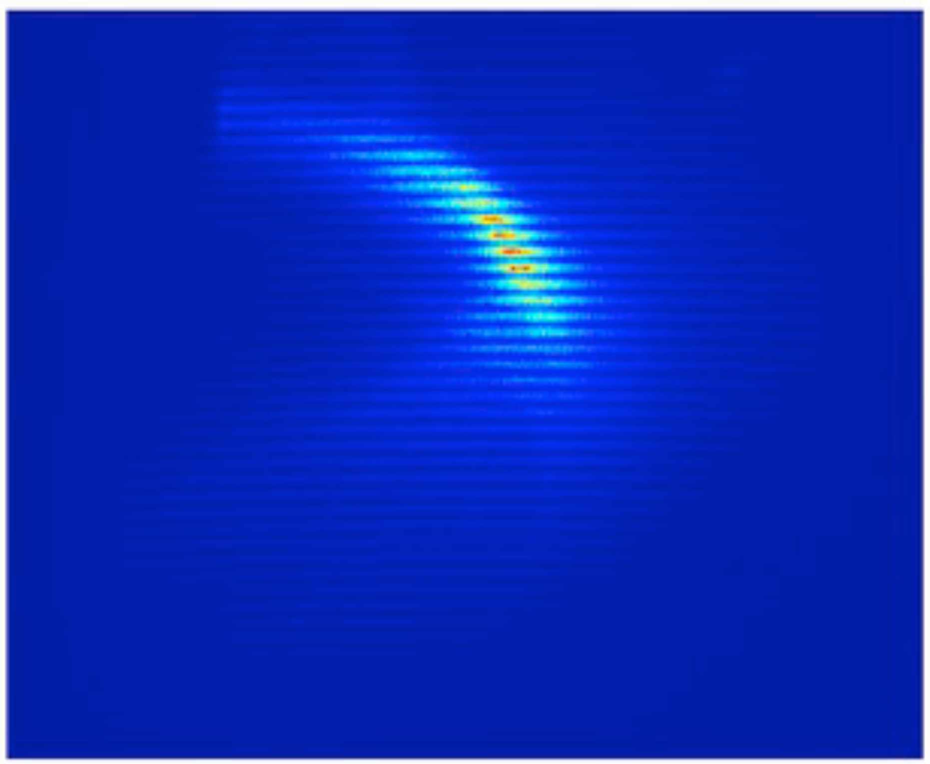

Demodulated Image: Phase shift

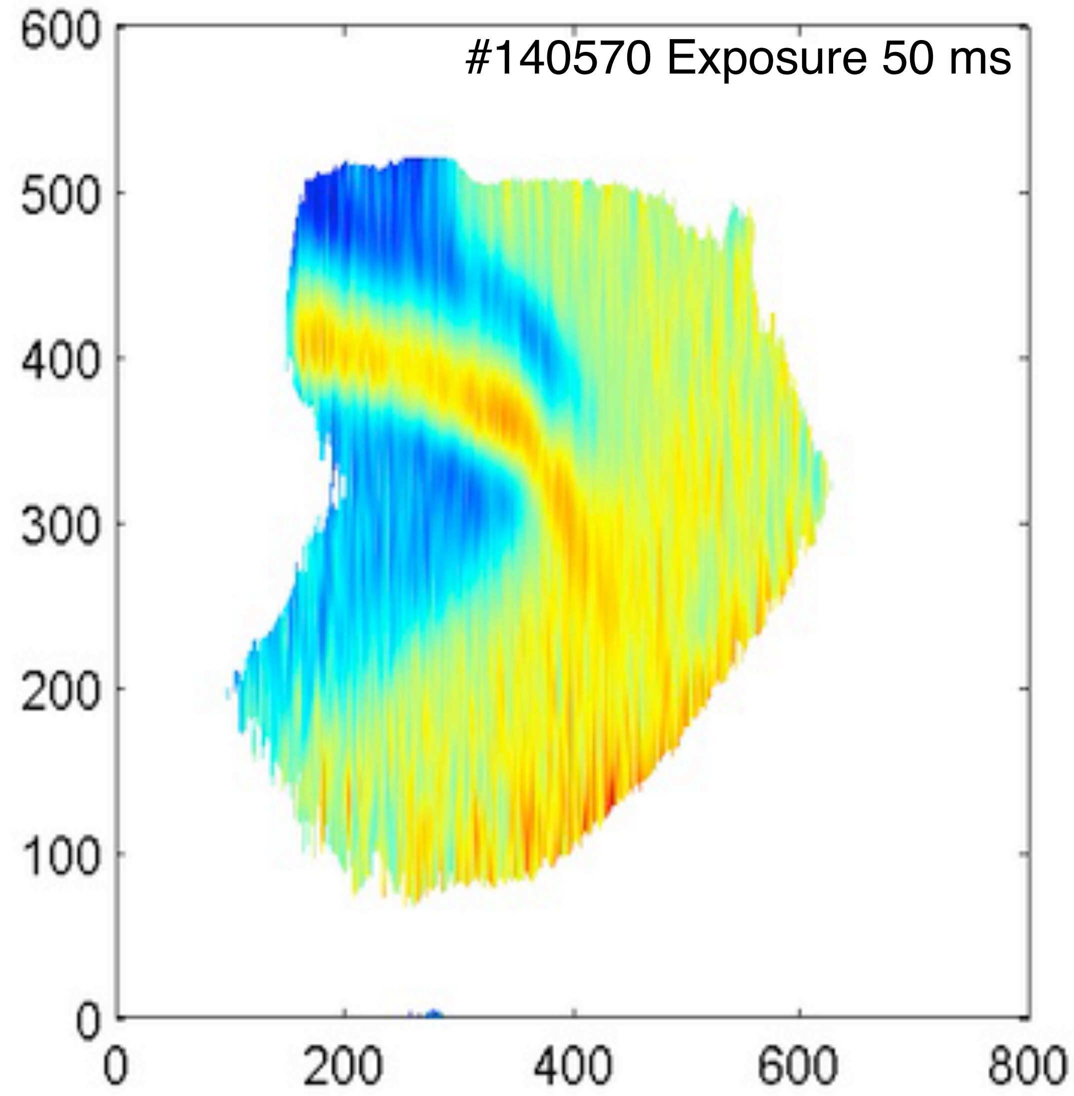

Reconstructed Brightness and Flow Profiles Conform with Equilibrium Surfaces

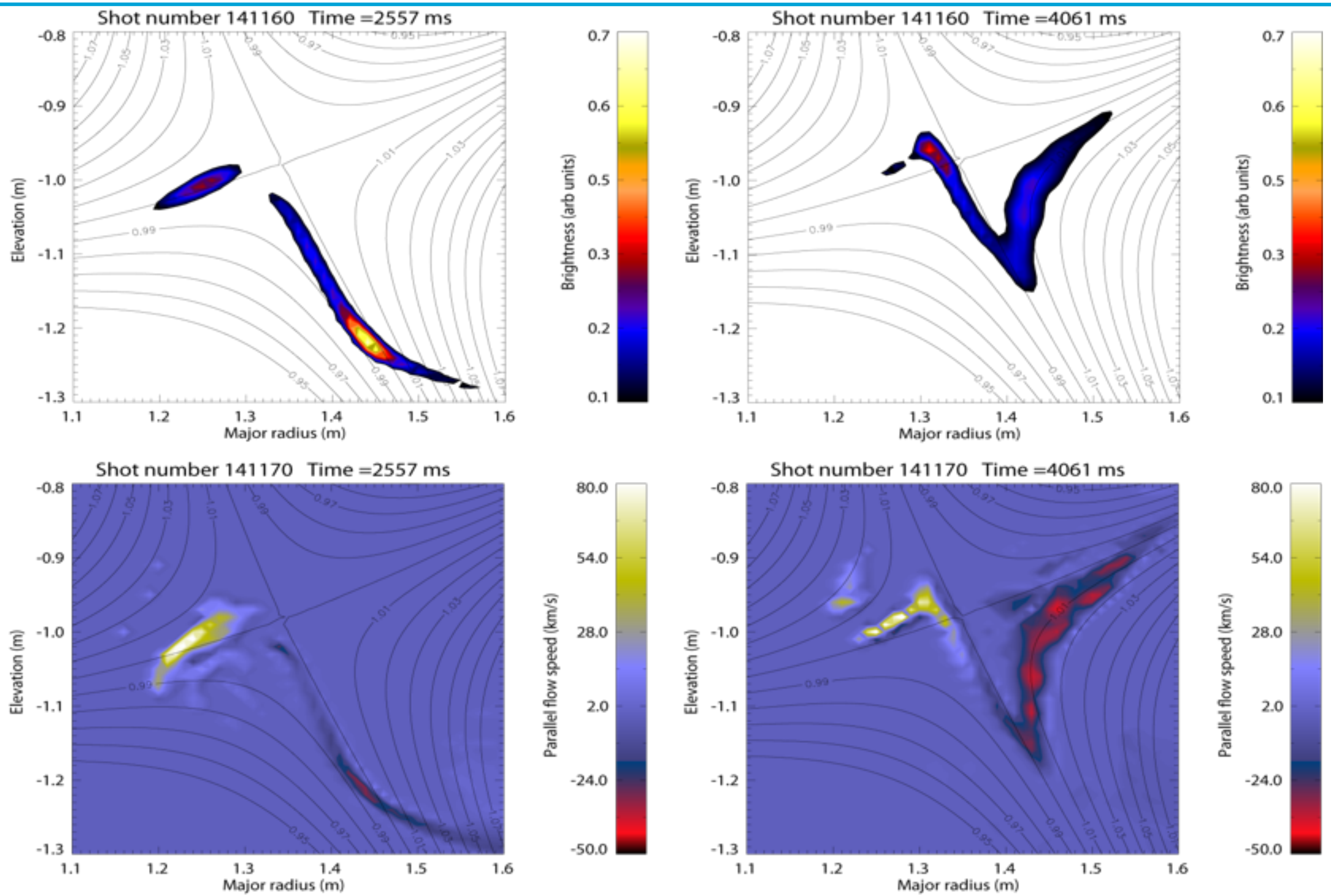

Monday, February 15, 2010

Short Summary/Outlook

- **First 2D flow pattern imaging using a polarization interferometer**
- Preliminary results show evidence of flow reversal with plasma current consistent with standard diagnostics
- Divertor imaging show complex flow structure of great interest for modelers
- Comparison with array of edge modeling codes

- Target multiple species for wider spatial coverage on NSTX
- Extension to Laser Induced Fluorescence- and Gas Puffing- assisted flow measurements are under investigation.

Key Components of Plasmas Generated in a Tokamak

Fueling

Heating

Current profile

Confinement

Core plasma

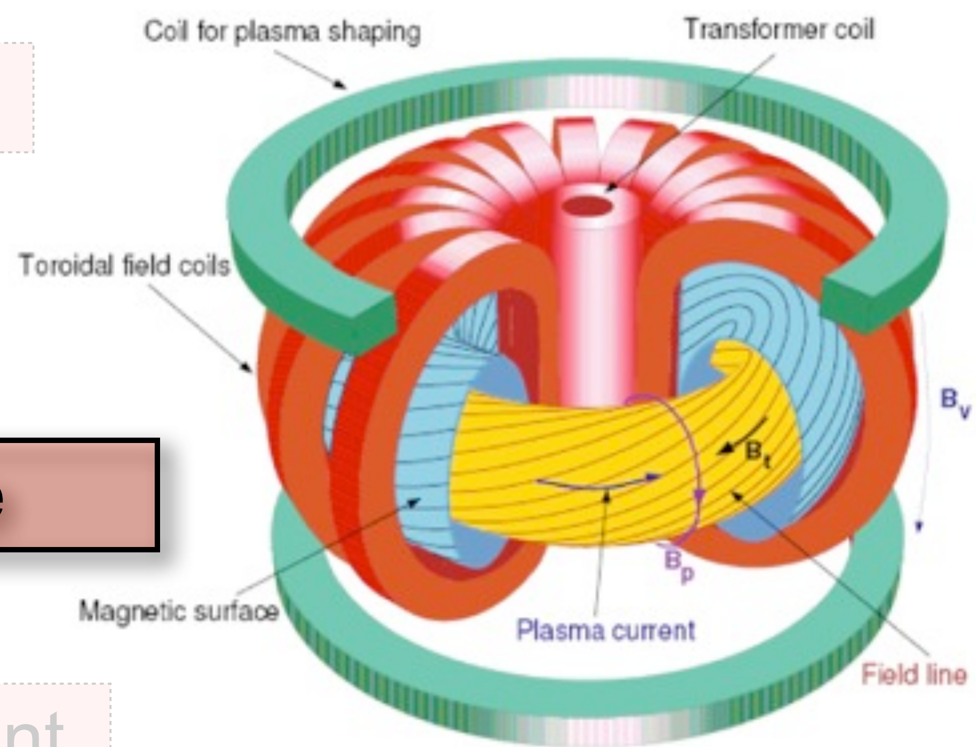

Stability & transport

Particle exhaust

Power exhaust

Plasma Facing Component loads

Impurity influx

(e.g., Flows)

Edge plasma

Motional Stark Effect enables Measurements of the Magnetic Field Pitch Angle

Injected beam atoms feel induced electric field in frame of the beam

Doppler shift from thermal H_α

$$\delta\lambda = \lambda_\alpha \frac{\hat{v_b} \cdot \hat{l}}{c}$$

Split by Stark effect

$$\Delta\lambda_s = 2.7574 \times 10^{-8}\ \mathrm{E}\ [\mathrm{nm}]\ \text{where}\ \mathrm{E} = |\vec{v_b} \times \hat{B}|$$

$$\vec{B} = \vec{B_\varphi} + \vec{B_\theta}$$

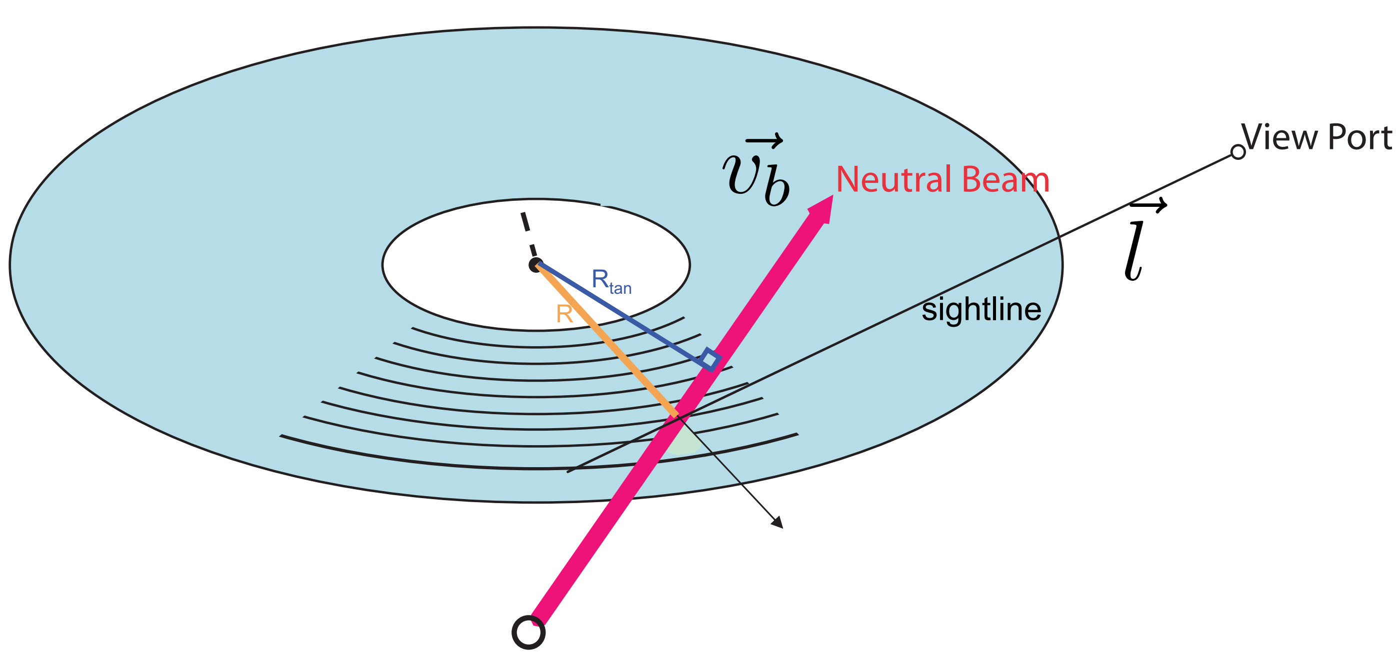

Measuring the polarization of the multiplet yields the orientation of the internal magnetic field

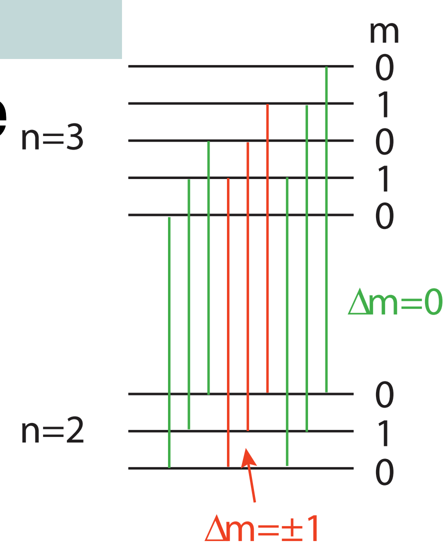

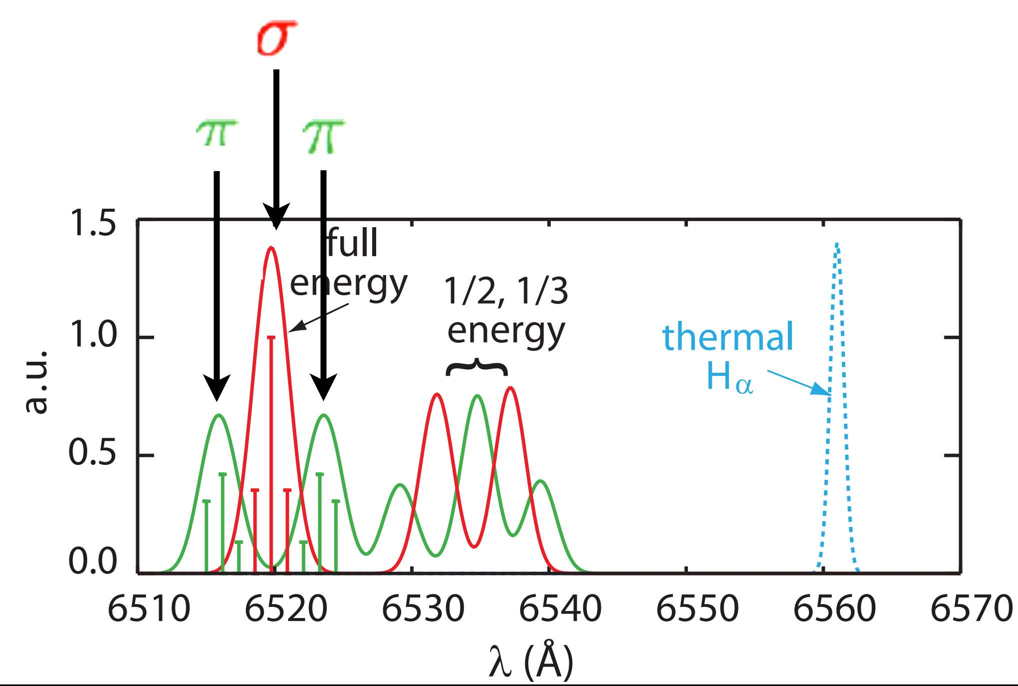

Shearing Polarization Interferometer Used to Encode Information of the Stark Multiplet

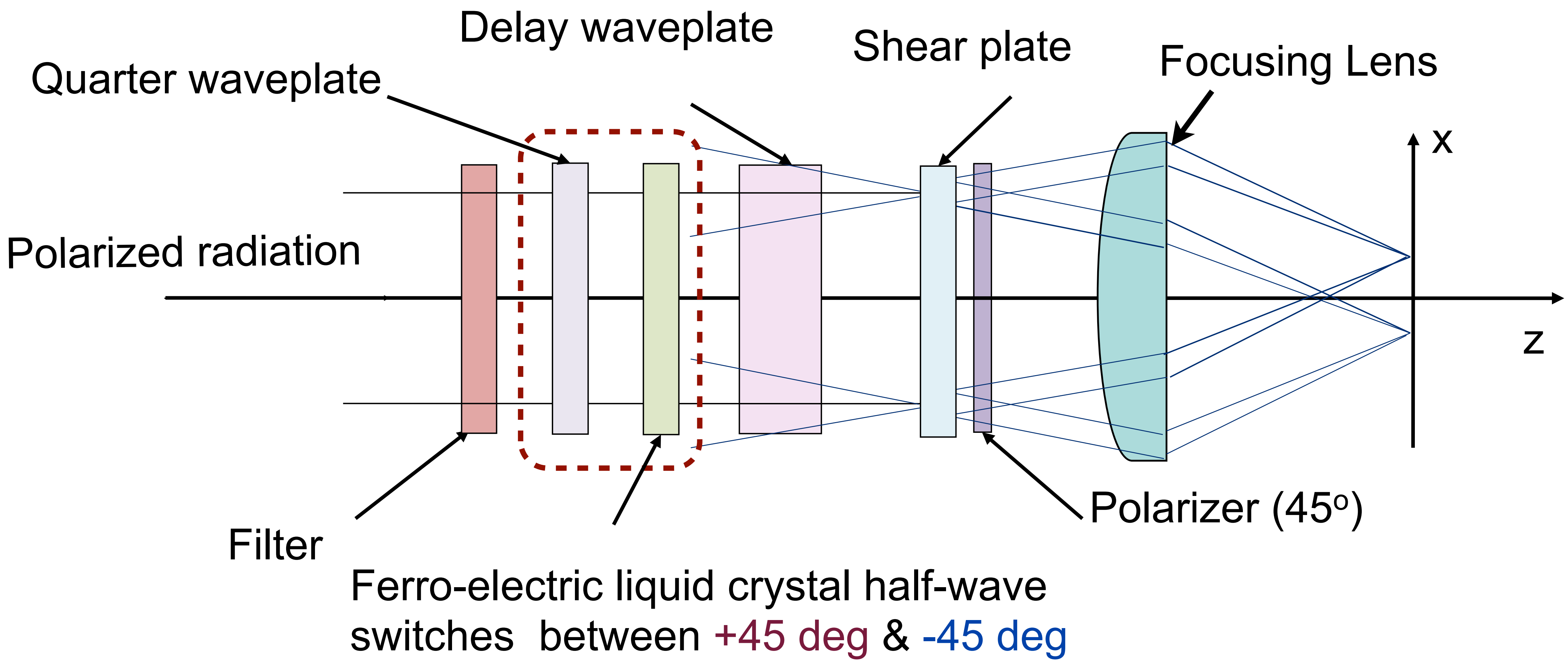

$$S = I[1 + \zeta cos(k_y y + \varphi + 2\theta)]$$

$$S = I[1 + \zeta cos(k_y y + \varphi - 2\theta)]$$

Image pair yields 4x the polarization angle

Outline

- How to image flows and the current profile?
  - Polarization interferometer
  - Spatial heterodyne system
- Applications
  - Imaging of Doppler flows (DIIID)
  - Magnetic field pitch angle map (TEXTOR)
- Summary and Outlook

Applications to Measuring the Magnetic Pitch Angle: TEXTOR Viewing Geometry

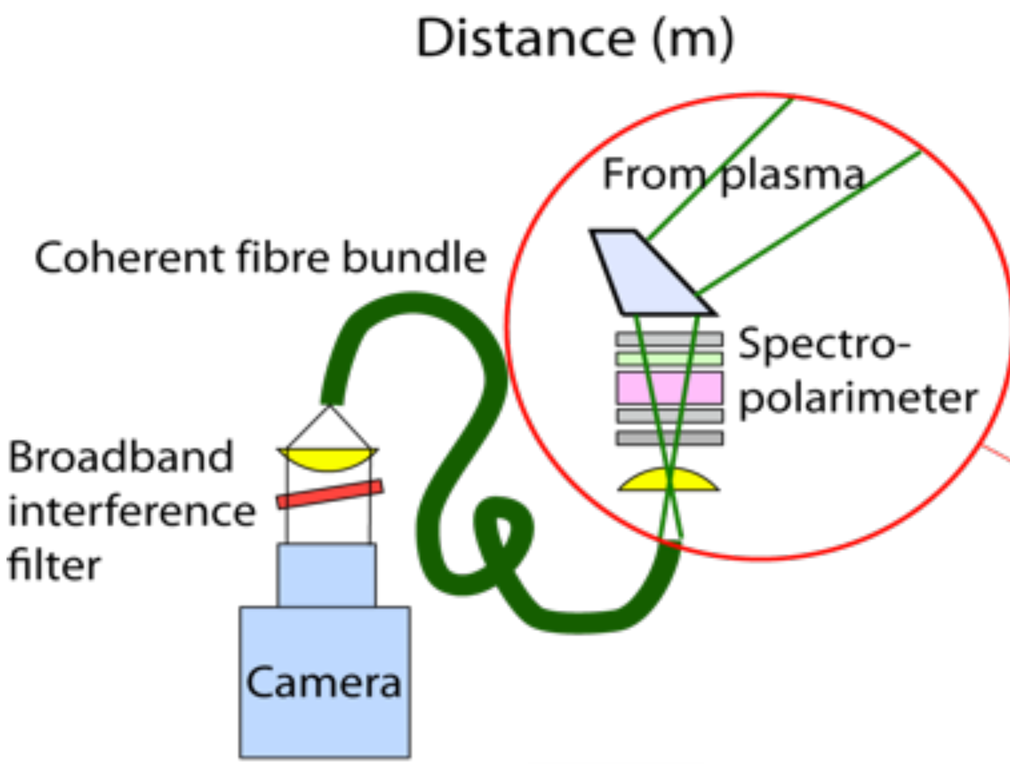

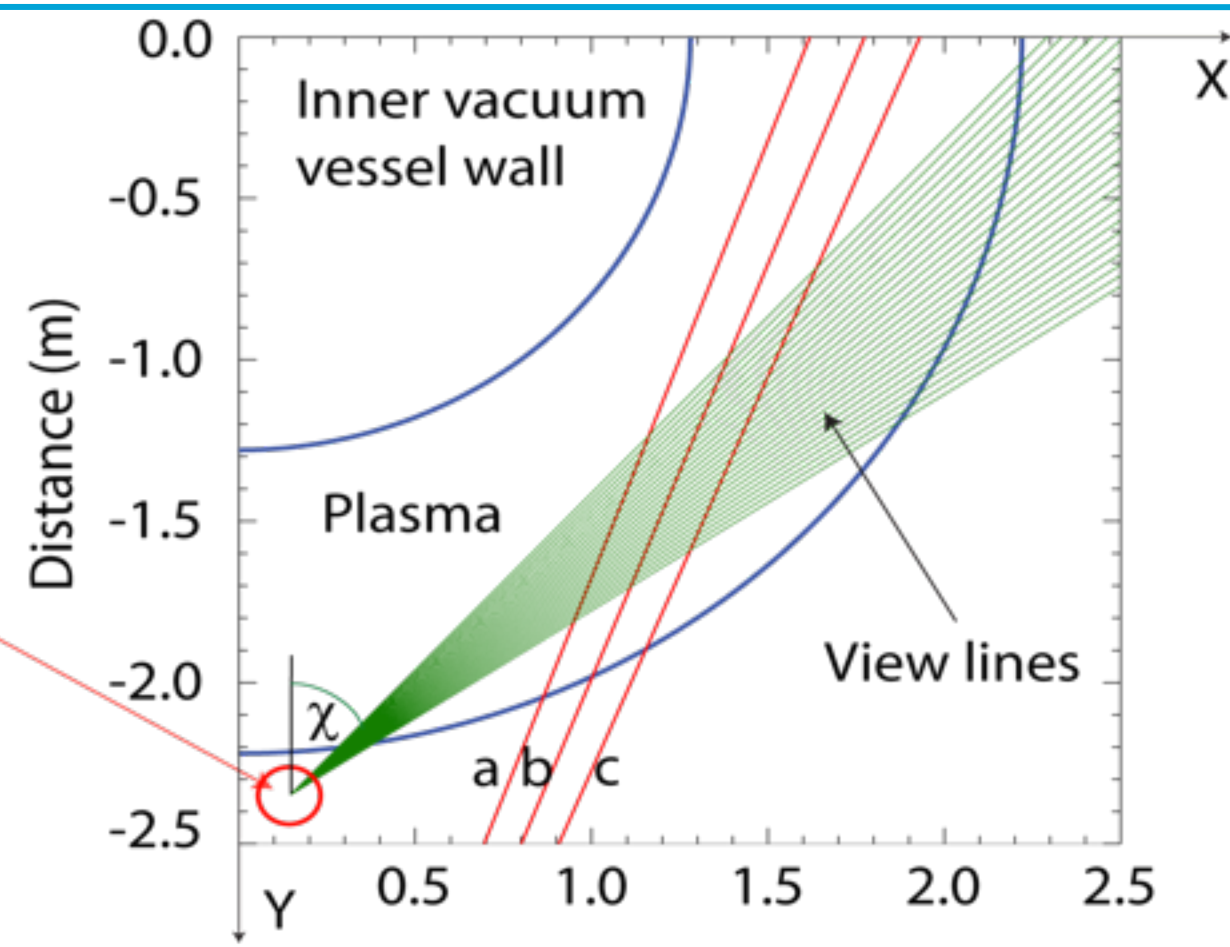

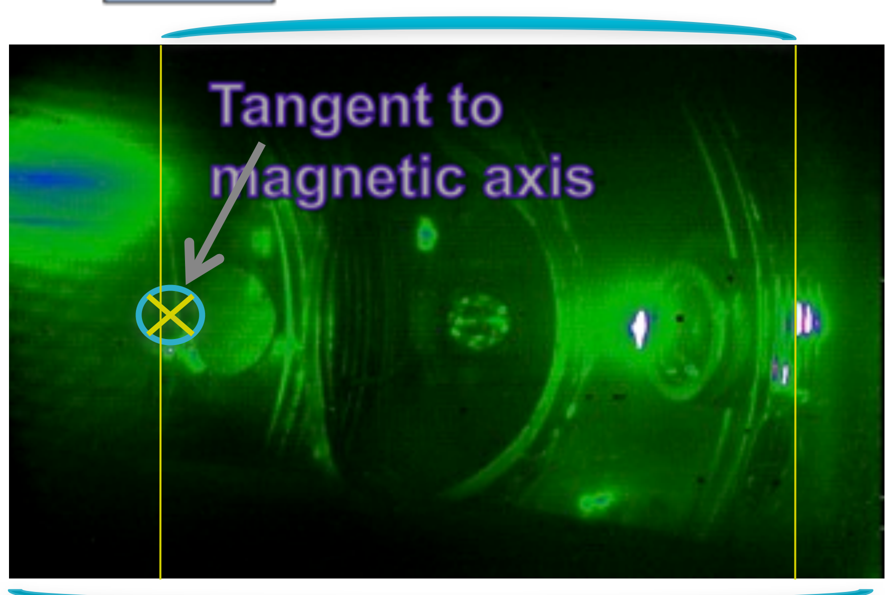

Beam
50 keV

Polarized Emission Generates Interference Fringes

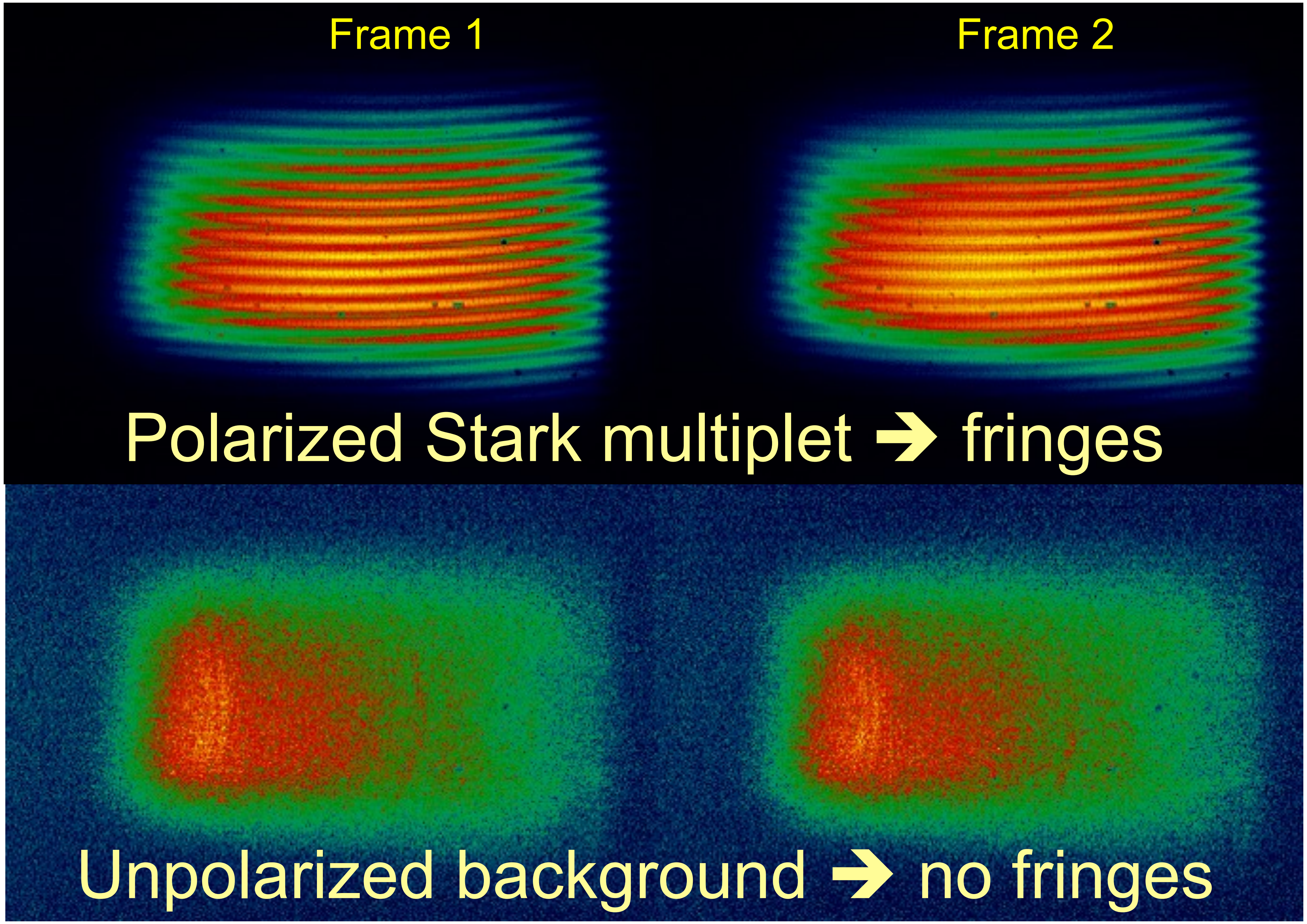

Beam on

Beam off

Interference Pattern: Beam Footprint Interferogram

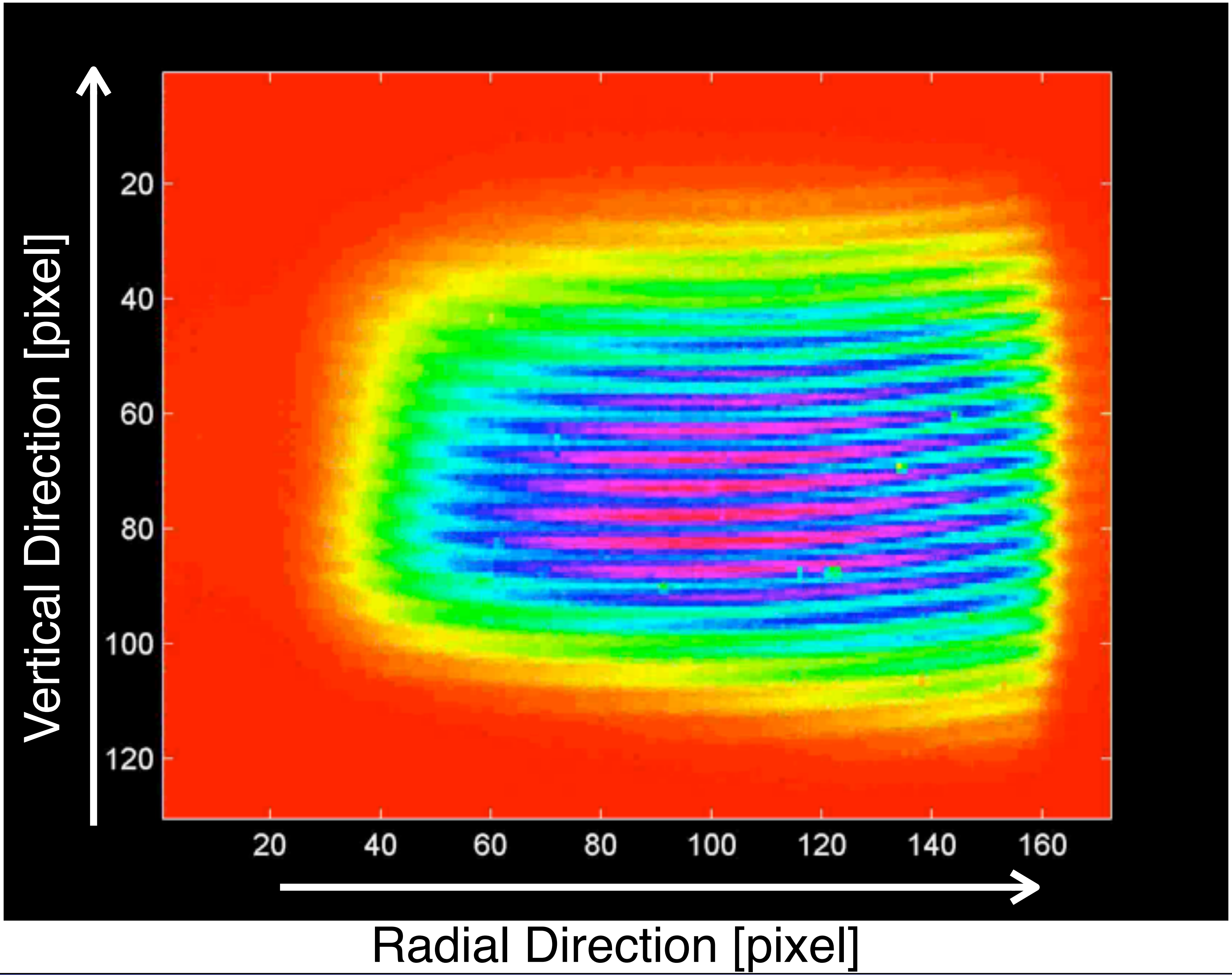

Image pair phase difference yields 4x polarization angle: Results

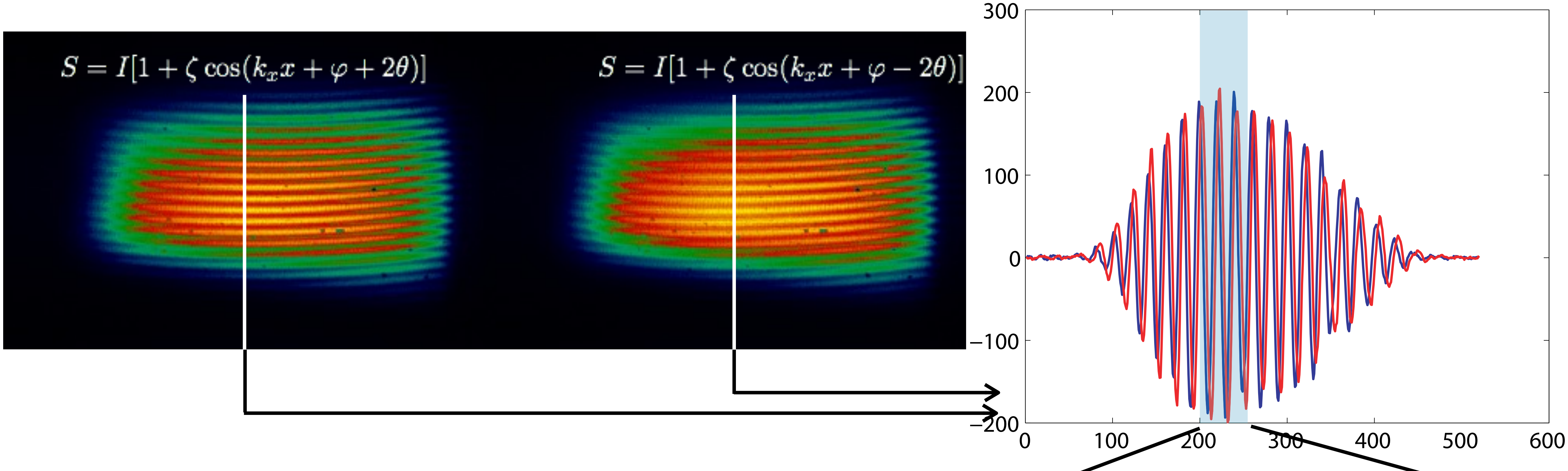

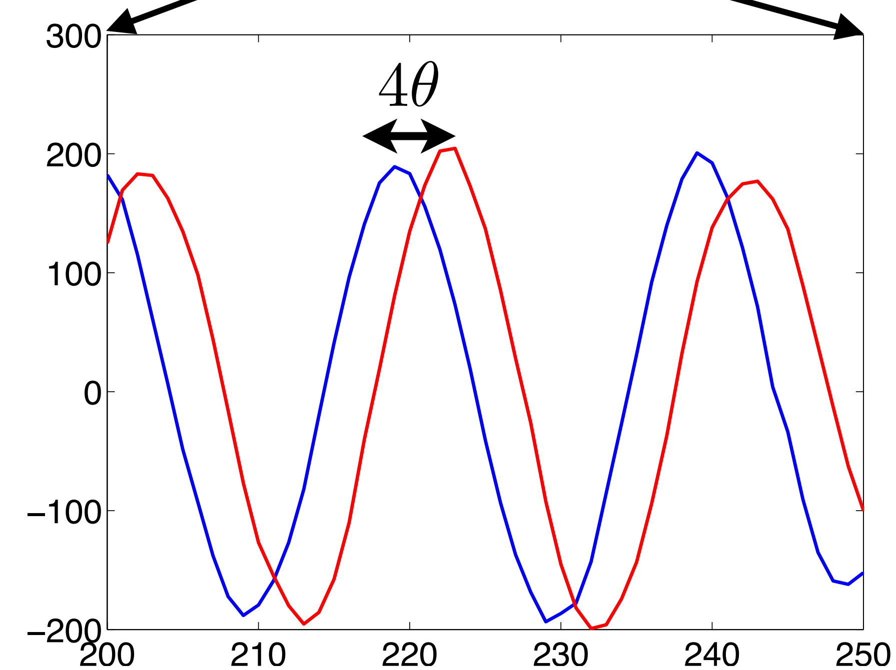

Spatial resolution Radial ~3mm Vertical ~15-20mm

Polarization angle resolution rms ~0.5 deg

2D Field Pitch Angle Map: Experiment and Simple Model

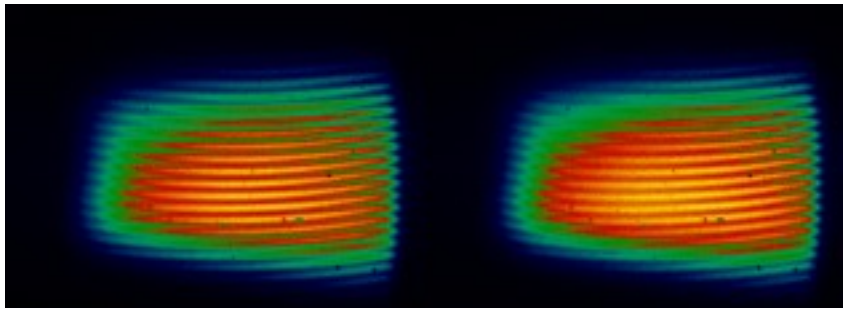

Spatial resolution Radial ~3mm Vertical ~15-20mm

Polarization angle resolution rms ~0.5 deg

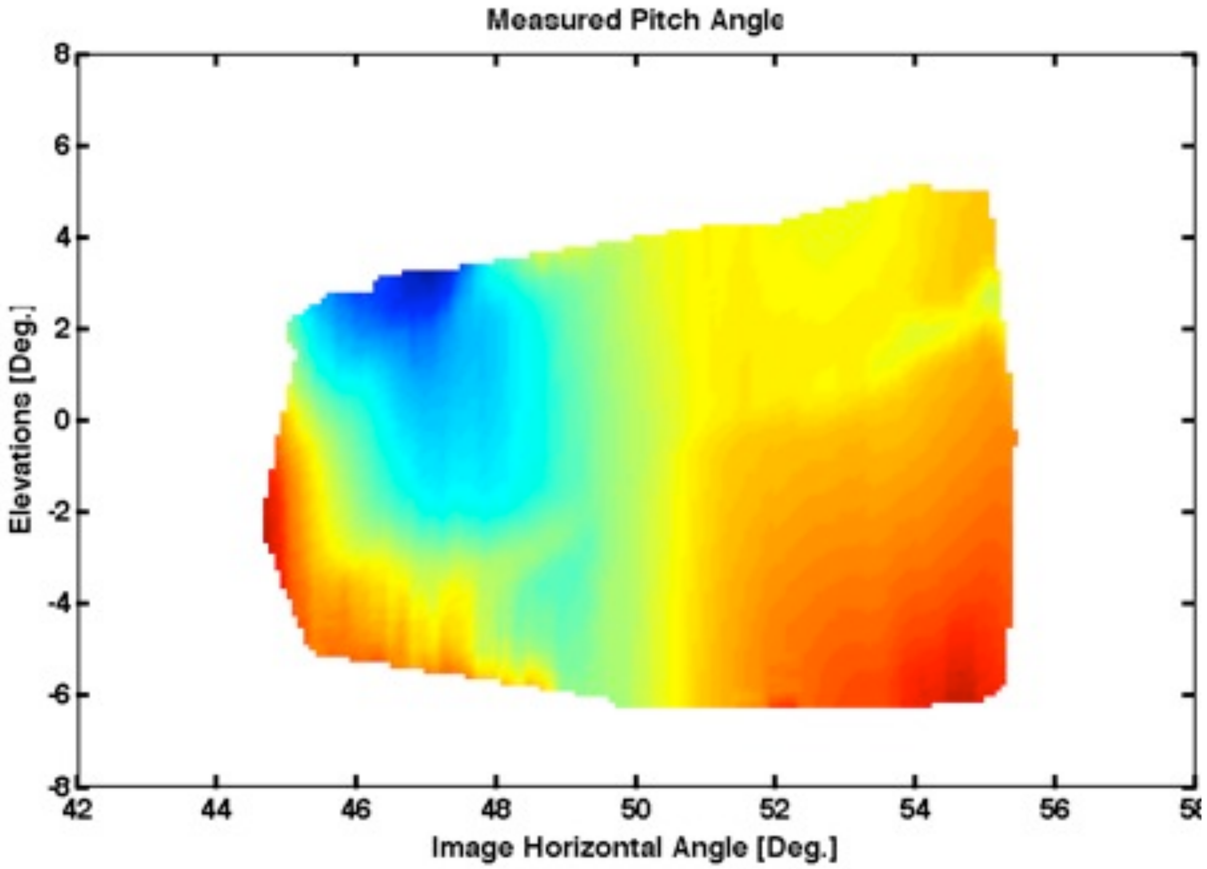

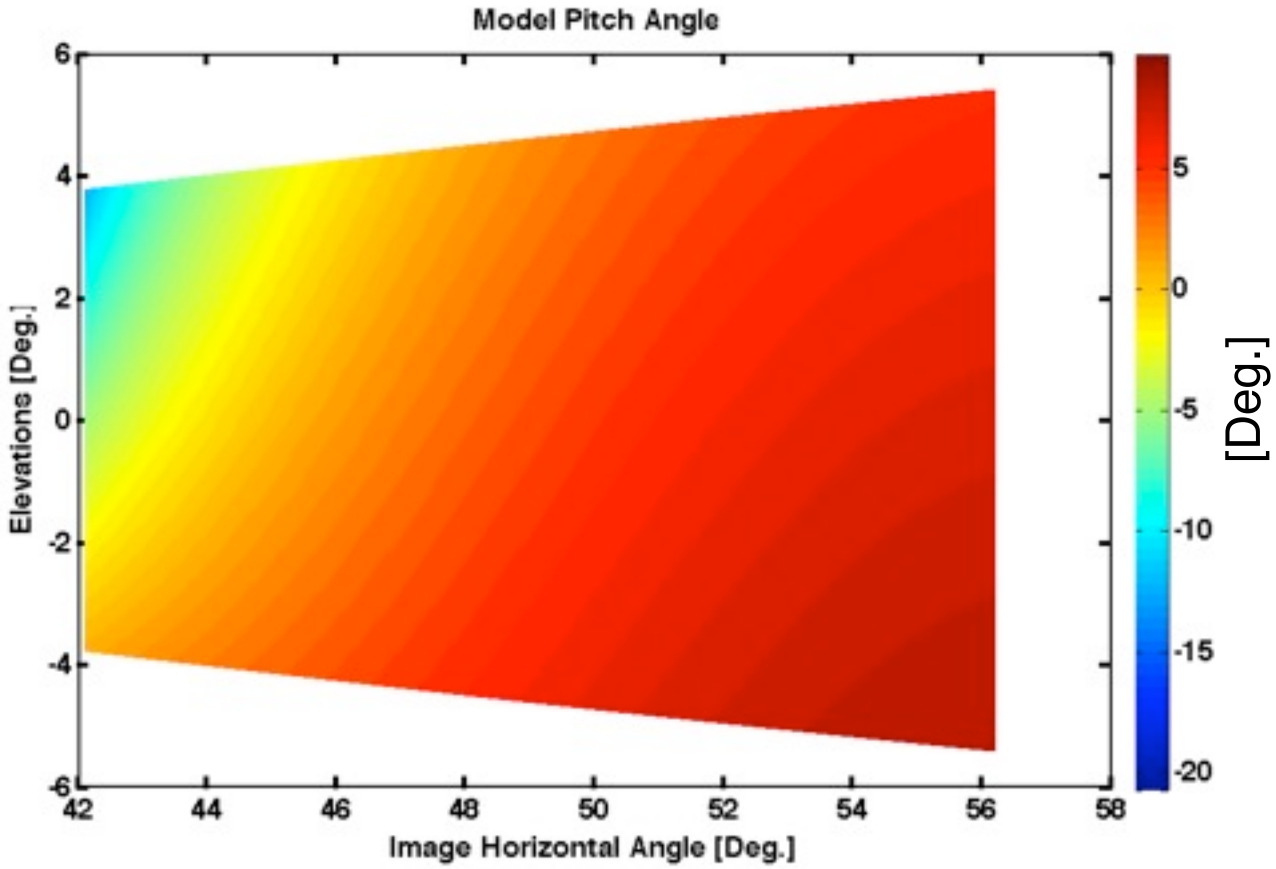

Discrepancies are due to imperfections of coupling prism

J. Howard, A. Diallo, R. Jaspers, and J. Chung Plasma and Fusion Research, **5**, S1010 ,(2010)

Beam Doppler Phase Shift: Experiment vs Model

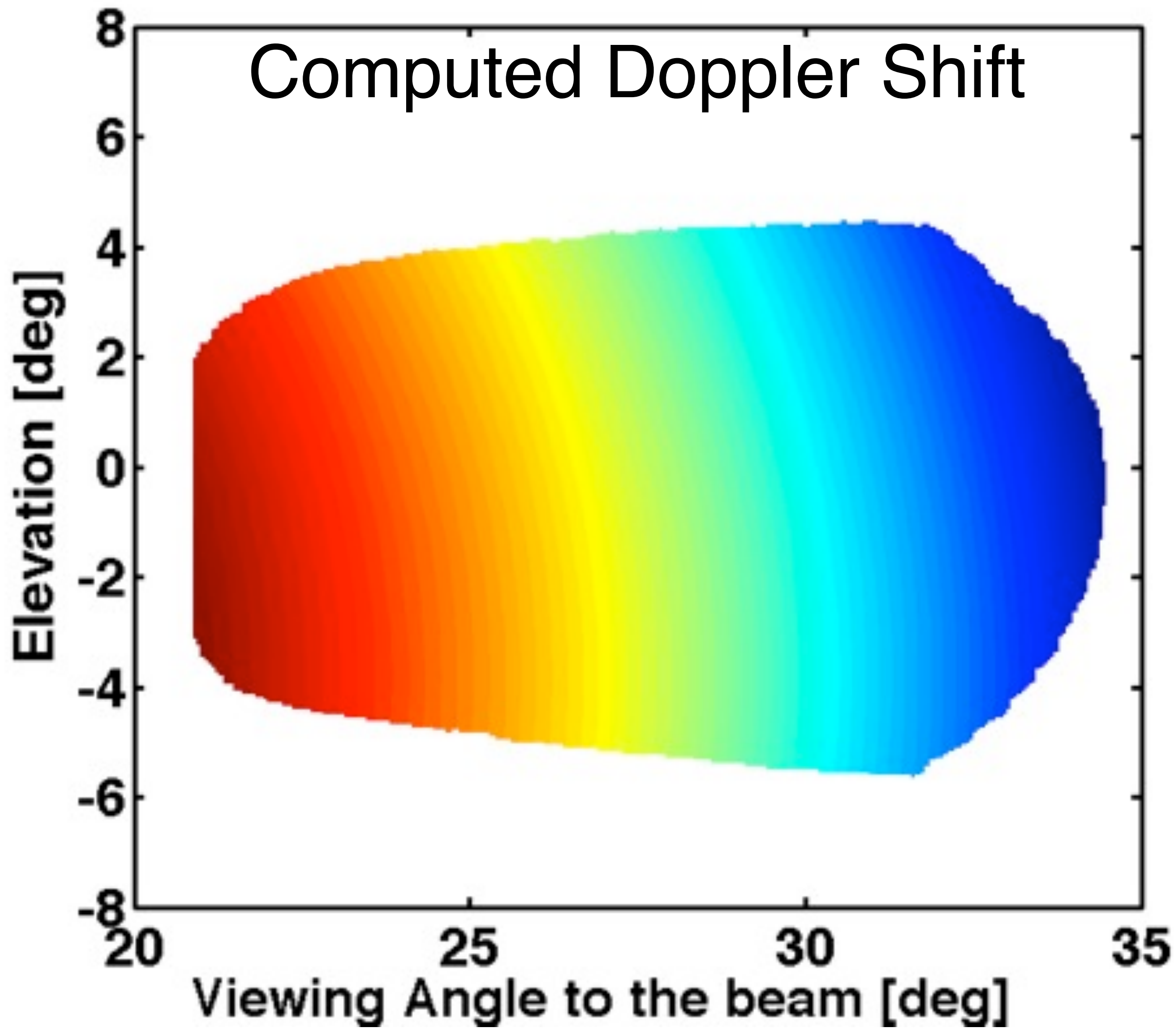

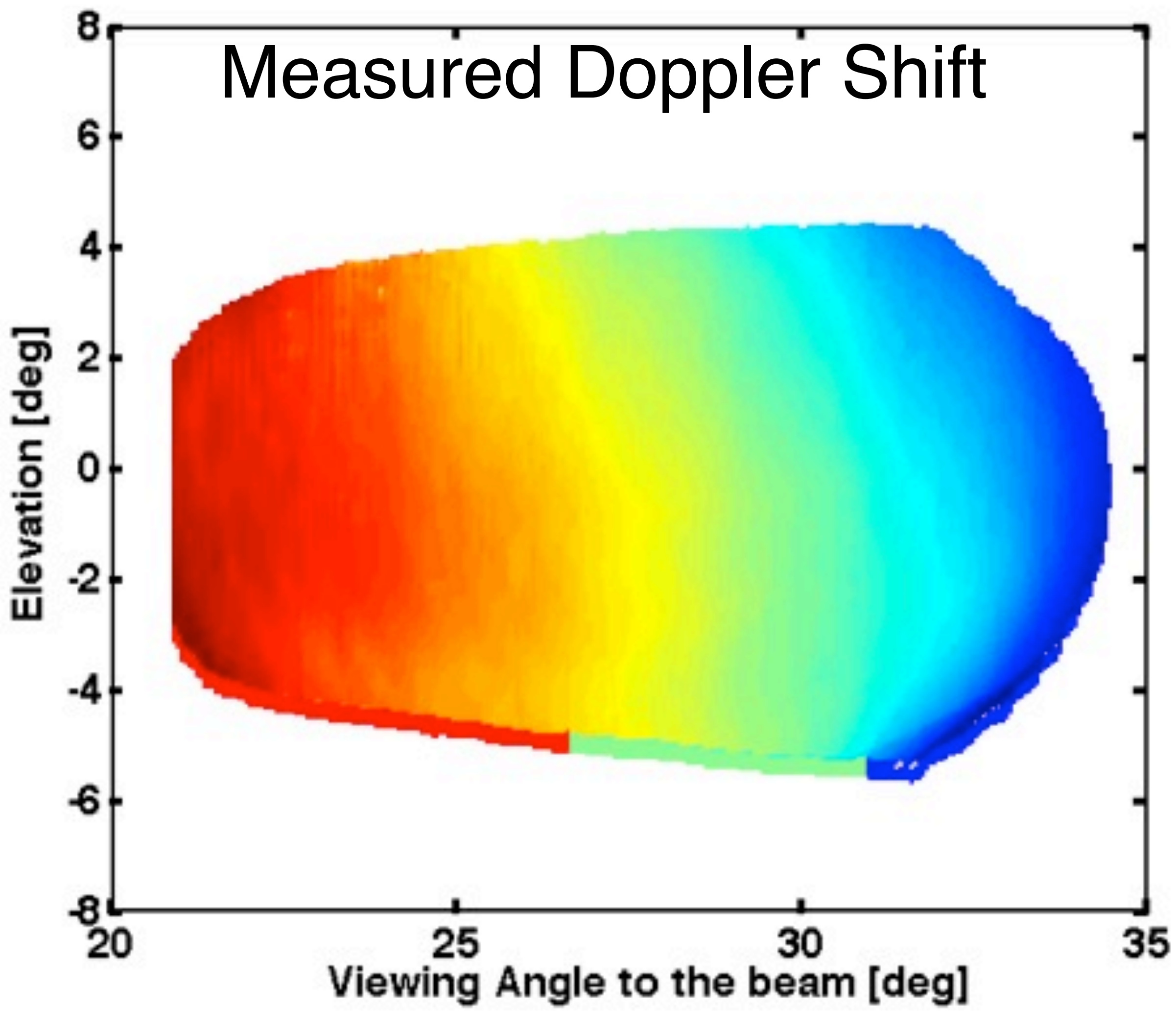

Agreement between Doppler shift and model

Summary and Next Steps

✓ Imaging provides a clear advantage over standard single point measurements

✓ First 2D pitch angle map qualitatively agrees with a simple model

Pitch angle map yields the current density profile

Important for plasma stability and fusion performance

✳ Next step: Applications of this imaging technique to resolve coherent events

✳ Extension to target Zeeman effects to image magnetic pitch in absence of neutral beams

✳ More work is required to obtain the flux function from the pitch map

✳ Extension to basic plasma devices ....

Backup Slides

Direct Measurement of the Flux Function

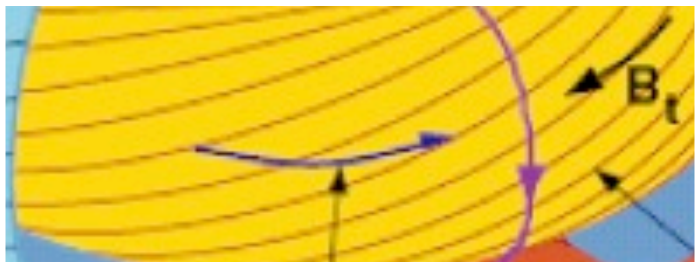

Plasma Current

Helical field line

Top view →

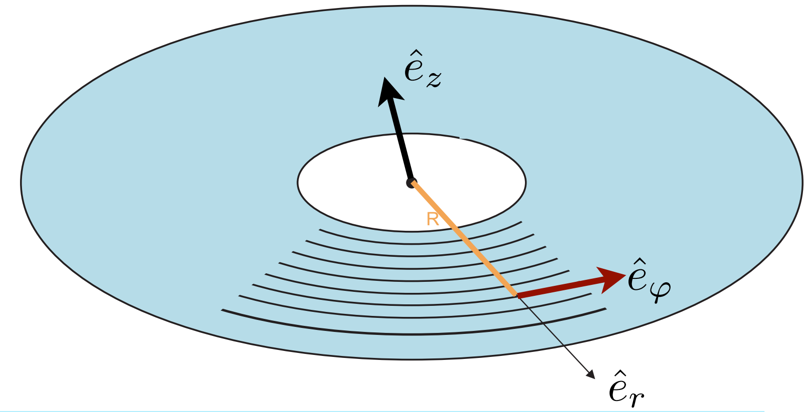

$$\tan\beta = \frac{A_1 B_z + A_2 B_r + A_3 B_\varphi}{A_4 B_z + A_5 B_r + A_6 B_\varphi}$$ where A_k are geometric factors.

Rewrite $S = B_z + \alpha B r$; Recall $\nabla \times B = \mu_0 J$

$$B_r = \frac{1}{r}\frac{\partial \psi}{\partial z} \text{ and } B_z = -\frac{1}{r}\frac{\partial \psi}{\partial r} \Rightarrow rS = \frac{\partial \psi}{\partial r} - \alpha \frac{\partial \psi}{\partial z}$$

$$\text{Let } u = r - z/\alpha,\ rS = \frac{\partial \psi}{\partial u} \Rightarrow \int rS du = \psi(u_2) - \psi(u_1)$$

2D pitch angle mapping enables the reconstruction of the magnetic flux function and the current profile.

Comparison with Charge Exchange Recombination Profile (CVI)

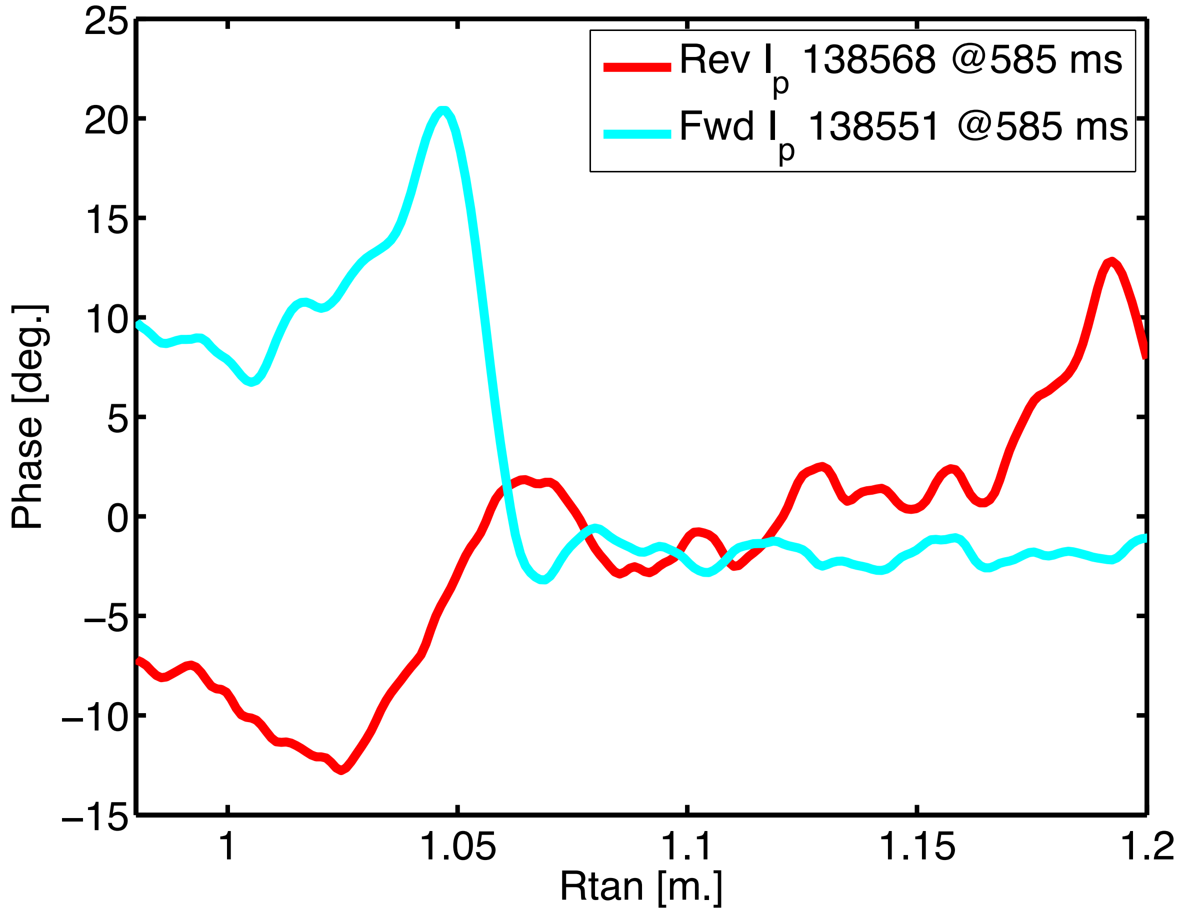

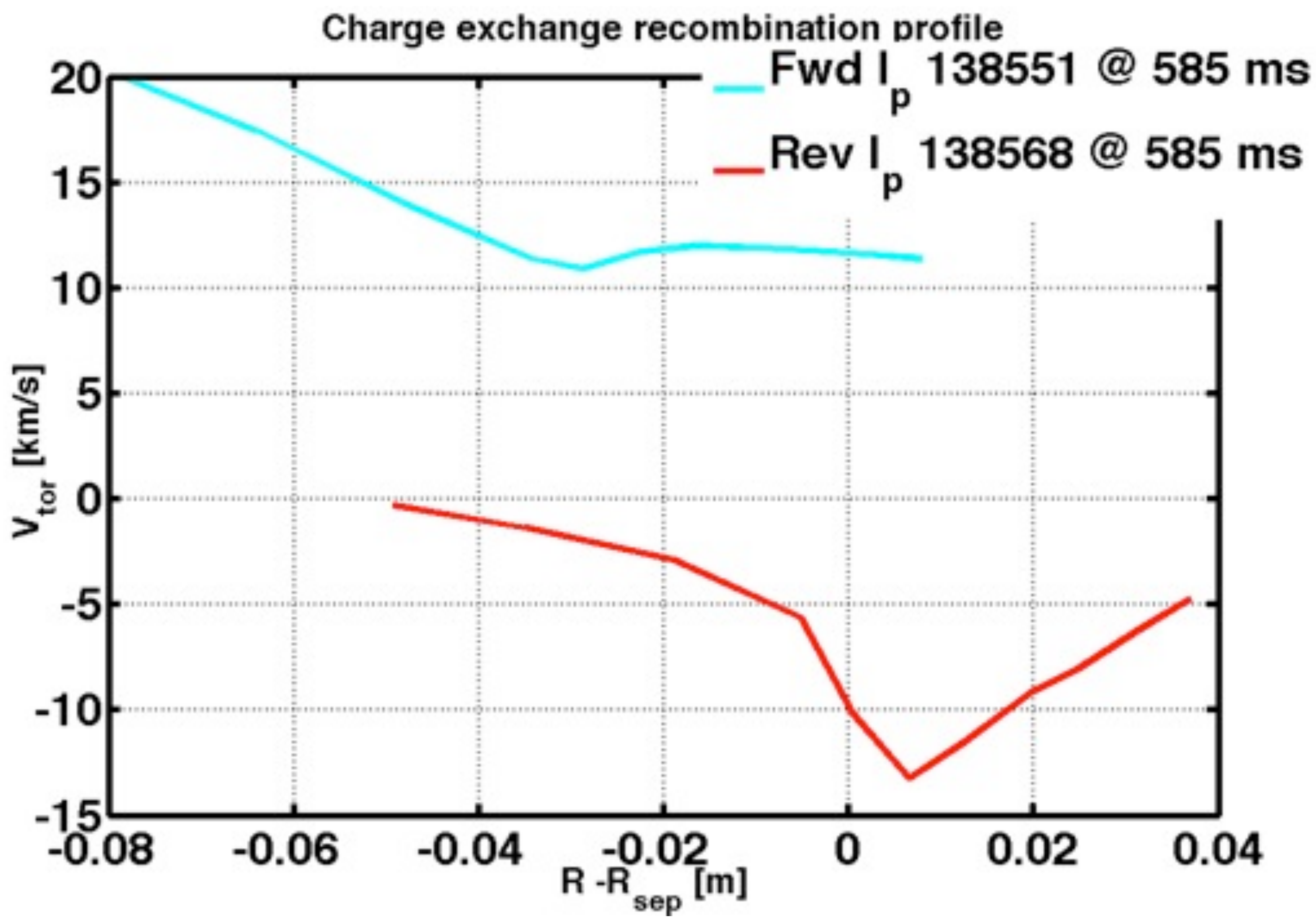

Sign reversal is consistent with standard measurements

Implementation of Doppler Imaging Instrument

$$I = \frac{I_0}{2}[1 + \zeta cos(\varphi_y + \varphi)]$$

$$\varphi = \frac{2\pi B(\lambda)L}{\lambda} \Rightarrow \varphi = \varphi_0(1 + \kappa\frac{\vec{v}\cdot\hat{l}}{c}) \quad \kappa = \frac{\lambda}{B}\frac{\partial B}{\partial \lambda}_{\|\lambda_0}$$